ROMA TRE
UNIVERSITÀ DEGLI STUDI

Scuola Dottorale in Biologia
Sezione "Scienze Biomolecolari e Cellulari"
Ciclo di Dottorato XXV

"Protein engineering for structure-function studies of bioactive (macro)molecules"

"L'ingegneria proteica nello studio della struttura e funzione di (macro)molecole"

A.A. 2012/2013

Candidato:
Dott.ssa Maria Carolina Spiezia

Docente Guida:
Prof. Fabio Polticelli

Co-tutor:
Dott. Cristiano Chiarabelli

Coordinatore:
Dott. Paolo Mariottini

Scientist is not who can give the real answers,

but who knows how to ask the right questions.

Strauss

ABSTRACT

The present Ph.D. project deals with the use of protein engineering techniques to express in recombinant form and characterize disulphide rich bioactive peptides, such as conotoxins. Moreover, taking advantage of their high target specificity and stability, the potential application of this class of macromolecules in “green” (environmental) and “white” (industrial) biotechnology fields have been explored.

Protein engineering is a powerful tool to improve some proteins parameters, acting on their sequence and structure, or to insert a desired function. There are three basic approaches in protein engineering: the *rational design* is an "intelligent" design that aims to change the structure or function of a protein, starting from the analysis of its three-dimensional structure. Its nucleotide sequence can be modified and the protein finally “built” and characterized (Hellinga, 1997). The second approach is the *directed evolution* or *DNA breeding*, a technique that simulates biological evolution mechanisms (Stemmer, 1994). In fact it involves the generation of random mutations in the gene coding for a protein, or shuffling the genes encoding different domains, to generate a high number of new proteins that will be then selected for a desired function. The third one, named *de novo* design, allows to design and build artificial proteins which don’t exist in nature, with novel functions and properties (Dahiyat and Mayo, 1997). This strategy takes advantage of computational biology to draw novel proteins both using natural scaffolds as templates and starting completely from scratch (Dahiyat and Mayo, 1997).

The idea of using stable protein structural motifs as scaffold for reproducing functional epitopes or stabilize bioactive conformations is currently one of the most successful approaches of protein engineering. The knottin family of proteins is particularly interesting from this point of view, since they share a common structural fold while having very different sequences and functions in animals and plants (Norton and Pallaghy, 1998). The multiple disulphide bridges that characterize this protein family give the greatest contribution to the structure stability, allowing a high variability of the remaining amino acid sequence regions. Among knottins, the highest tolerance to sequence variability is observed in conotoxins, small disulphide-rich neurotoxic peptides extracted from cone snails venom. Nature, during the evolution, has engineered this stable scaffold to express a great variety of neurotoxins with a remarkable high target specificity for different ion channels, both voltage-gated and ligand-gated (Olivera and Teichert, 2007). As a result, their scaffold represents an excellent starting

point for design strategies aimed at developing new miniproteins with new properties as well as more stable/active conotoxins for therapeutics (Clark et al., 2005).

From the natural source, the purification of conotoxins proved to be very difficult because of the large number of specimens needed to obtain a sufficient amount of venom to process. Thus, during this thesis work, a recombinant expression system has been developed to express conotoxins as GST-fusion proteins, overcoming both the problem of the small amount of a single conotoxin that can be extracted from the *Conus* venom, and their propensity to form insoluble aggregates because of the formation of intermolecular disulfide bridges. As a test case, the new protocol has been used to express conotoxin Vn2 from the Mediterranean Sea *Conus ventricosus*, a 33 amino acids long highly hydrophobic neurotoxic peptide, and its Asp2His mutant (Spiezia et al., 2012). This first part of the work involved cloning of both the conotoxins in pET-CM plasmid and their purification by affinity chromatography, exploiting the GST tag. Since the worm-hunting *C. ventricosus* has an array of toxins acting on invertebrate ion channels, GST-conotoxins have been tested for their neurotoxic activity on the larvae of the moth *Galleria mellonella*, taken as an insect model system (Spiezia et al., 2012). Further, using ω-conotoxin GVIA as template, novel metal-binding peptides were designed to generate novel biocatalysts. Through computational modeling, two disulphide bridges in the original conotoxin have been replaced with His residues and the redesigned peptides, named Cupricyclin-1 and Cupricyclin-2, have been synthesized and characterized for their copper binding ability and superoxide dismutase activity (Barba et al., 2012). The last part of the work concerned the generation of Cupricyclin-1 mutants with the aim to improve its superoxide dismutase activity and to change metal-binding specificity from copper to iron and manganese. The new expression system developed in the first part of the present project was successfully used to express these Cupricyclin mutants as GST-fusion proteins. Following GST tag removal using thrombin cleavage, the mutants have been purified and their metal binding properties analyzed by optical and fluorescence spectroscopy and mass spectrometry.

Further studies will be necessary to elucidate the redox properties of these novel Cupricyclins and their potential as biosensors for the detection of heavy metals or as therapeutics in oxidative stress injuries, given the ability of Cupricyclin-1 to dismutate O_2^- radicals.

RIASSUNTO

Il presente progetto di dottorato si propone di utilizzare le tecniche dell'ingegneria proteica per esprimere in forma ricombinante e caratterizzare peptidi bioattivi ricchi in ponti disolfuro, quali le conotossine. Sfruttando la loro alta specificità di target e struttura stabile, sono state esplorate le loro potenziali applicazioni sia nel campo delle biotecnologie cosiddette "verdi" (ambientali) che "bianche" (industriali). L'ingegneria proteica è un potente strumento con il quale è possibile modificare le proprietà delle proteine, agendo sulla loro sequenza o sulla loro struttura, o dotarle di nuove funzioni. L'ingegneria proteica prevede tre approcci principali: il è un "intelligente" che mira a modificare la struttura o la funzione di una proteina, partendo dalla analisi della struttura tridimensionale. La sua sequenza nucleotidica può essere modificata e infine la proteina può essere "costruita" e caratterizzata (Hellinga, 2007). Il secondo approccio è l'*evoluzione diretta* (Stemmer, 1994) che simula l'evoluzione biologica. Infatti questa tecnica comporta la generazione di mutazioni casuali nel gene codificante per una data proteina, o il riarrangiamento dei geni codificanti domini differenti, per generare un gran numero di nuove proteine che saranno poi selezionate per la funzione desiderata. La terza strategia, chiamata *de novo design*, permette di progettare e costruire proteine artificiali che non esistono in natura, con nuove funzioni e proprietà (Dahiyat e Mayo, 1997). Questa strategia si avvale della biologia computazionale per progettare nuove proteine, sia utilizzando come stampo motivi strutturali già esistenti in natura sia partendo completamente da zero (Dahiyat e Mayo, 1997). L'idea di utilizzare motivi strutturali proteici stabili come impalcatura per la riproduzione di epitopi funzionali o stabilizzare conformazioni bioattive è attualmente uno degli approcci di maggior successo dell'ingegneria proteica. La famiglia proteica delle "knottins" è particolarmente interessante sotto questo punto di vista, dal momento che i membri di questa famiglia condividono una stessa struttura di base pur avendo sequenze e funzioni molto diverse nelle piante e negli animali, (Norton e Pallaghy, 1998). I ponti disolfuro che caratterizzano queste proteine danno il maggior contributo alla stabilità della struttura, consentendo la variabilità della restante sequenza amminoacidica. Tra le "knottins", la maggior tolleranza alla variabilità della sequenza si riscontra nelle conotossine, piccoli peptidi neurotossici ricchi in disolfuri presenti nel veleno dei molluschi del genere *Conus*. La Natura, nel corso dell'evoluzione, ha utilizzato questa struttura stabile per esprimere una grande varietà di neurotossine con un'alta

specificità di bersaglio per diversi canali ionici, sia voltaggio che ligando dipendenti (Olivera and Teichert, 2007). Di conseguenza, lo "scheletro" delle conotossine rappresenta un ottimo punto di partenza per strategie di progettazione volte a sviluppare nuove mini proteine con nuove proprietà o conotossine più stabili o attive come agenti terapeutici (Clark et al., 2005). La purificazione delle conotossine partendo direttamente dalla sorgente naturale si è rivelata molto difficile a causa del grande numero di esemplari necessari per ottenere una quantità sufficiente di veleno. Per aggirare questo problema è stato sviluppato un sistema di espressione ricombinante per esprimere le conotossine come prodotti di fusione legati alla glutatione-S-transferasi (GST). Questo approccio ha permesso di ovviare anche alla loro propensione a formare aggregati insolubili dovuti nella maggior parte dei casi alla presenza di ponti disolfuro intermolecolari. Il nuovo protocollo è stato utilizzato per esprimere la conotossina Vn2 del veleno del *Conus ventricosus*, un neuropeptide formato da 33 aminoacidi e altamente idrofobico, e il suo mutante Asp2His (Spiezia et al., 2012). Questa prima parte del lavoro ha previsto il clonaggio di entrambe le sequenze nucleotidiche delle conotossine nel plasmide pET-CM e la loro purificazione mediante cromatografia di affinità sfruttando la GST. Predando policheti marini, il veleno del *C. ventricosus* contiene tossine che agiscono sui canali ionici di invertebrati. Per questo motivo l'attività biologica delle conotossine espresse in forma ricombinante fuse alla GST è stata studiata utilizzando come sistema modello le larve della camola del miele *Galleria mellonella* (Spiezia et al., 2012). Successivamente, utilizzando come stampo un'altra conotossina molto ben caratterizzata, l'ω-conotossina GVIA, sono stati progettati peptidi leganti rame con l'obiettivo di ottenere dei biocatalizzatori. Mediante modellistica molecolare, due dei tre ponti disolfuro presenti nella conotossina originaria sono stati sostituiti con quattro residui di istidina ed i peptidi ridisegnati, denominati Cupricyclin-1 e Cupricyclin-2, sono stati sintetizzati e caratterizzati per la loro capacità di legare ioni rame e di catalizzare la dismutazione di anioni superossido (Barba et al. , 2012). L'ultima parte del lavoro ha riguardato la generazione di mutanti del peptide Cupricyclin-1 con lo scopo di migliorarne l'attività superossido dismutasica e modificarne la specificità di legame dal rame al ferro e/o manganese. Il nuovo sistema di espressione sviluppato nella prima parte del presente progetto è stato utilizzato con successo per esprimere i mutanti della Cupricyclin-1 come proteine di fusione alla GST. Una volta eliminato il *tag* mediante digestione con trombina e trattamento ad alte temperature, i nuovi peptidi sono stati caratterizzati mediante spettroscopia ottica, di fluorescenza e spettrometria

di massa. Una comprensione dettagliata delle loro proprietà catalitiche sarà necessaria per poterne esplorare le applicazioni come biosensori per la rilevazione di metalli pesanti, nonché come agenti terapeutici per malattie da stress ossidativo data la loro capacità di dismutare anioni superossido.

INDEX

1. INTRODUCTION

Protein engineering is a young discipline, born in the early 1980's combining different experimental approaches, such as biological, chemical and computational, to modify proteins structure with the goal to improve some functional parameters or to insert desired functions (Ulmer, 1983). It has been proved to be an absolutely essential tool, both in basic research, for example to increase our basic understanding of protein structure-function relationships, and in applied sciences, such as in the biotechnology field. In recent years in fact, the use of engineered (macro)molecules has been growing in all areas of biotechnology, from the pharmaceuticals to the green chemistry fields, from the industrial to more innovative fields such as the research on biofuels and biomaterials (Wargacki et al., 2012; Chow et al, 2008). Protein engineering has become a key method to improve enzymes and proteins properties or even to design molecules with novel functions to obtain best performance with reduced costs and with a very low environmental impact (Cao et al., 2009).

The fundamentals of protein engineering rely on the fact that proteins consist of a linear chain of amino acids, which in the most cases fold in a unique and well defined three-dimensional structure with a specific function. Therefore the amino acid sequence is the starting point to modify or generate "ex novo" functions. There are two basic approaches: the *rational design* makes use of detailed information on the three-dimensional structure and function of a protein to modify its amino acid sequence, to affect its functional properties (Hellinga, 1997). *Rational design*, though not always successful, allows to change a protein structure in a predictable way and it's a relatively inexpensive process. However it requires detailed structural information on the protein which sometimes are not available. Moreover, even if all the protein structural features are known it is difficult to predict which amino acid substitution will generate the functional change. Therefore this strategy requires many cycles of modification and testing to produce an engineered protein with the desired properties.

Directed evolution or *DNA breeding* (Stemmer, 1994), does not need a full structural map and involves generating random mutations in the gene encoding a protein, or shuffling the genes encoding different sequences, to generate a high number of novel proteins which are then subjected to selection for a desired function. Through repeated rounds of mutation and selection, it is possible to accelerate the evolution of the desired properties,

somehow mimicking the evolution and selection process that is the corollary of the variability. However, *directed evolution* is often time consuming and expensive, because each new protein combination has to be tested for the selected function. The results achieved through *rational design* and *directed evolution*, along with the advancement in computer technologies have led to the development of a third strategy to design and build artificial proteins not existing in nature, with novel functions and properties. The challenge of this approach, named *de novo design* (Dahiyat and Mayo, 1997) is to draw an amino acid sequence leading to a thermodynamically stable structure to ensure a specific function. For this purpose, proteins with the desired activity and a well characterized active site and three dimensional structure are used as templates. These information are then integrated with theoretical knowledge on protein folding rules and computational biology models. The last ones have become a powerful tool in the *de novo design* strategy because i) the advanced algorithms used allow to find the lowest energy folded sequence-structure combination and ii) they allow to evaluate the effect of an amino acid change on the protein structure and function, providing a guideline in the design process (Dahiyat and Mayo, 1997; Baker, 2006). Currently the strategies to improve proteins properties or to create new ones involve combined elements of the three approaches, even if each of them has a different starting point, works in different ways and with different tools.

1.1 Rational design

Willem Stemmer, the father of *directed evolution*, and Brett Holland wrote: "Rational design, also known as computer modeling, attempts to modify or create [protein] molecules for specific applications by predicting which amino acid sequence will produce a protein with the desired properties" (Stemmer and Holland, 2003). Therefore, *rational design* is an "intelligent" design which aims to change the structure or function of a protein, according to well-defined criteria, *i.e.* knowing the result to obtain, which is the best strategy to use and which kind of changes is needed to pursue. This strategy requires knowledge of the three-dimensional structure of the desired protein; starting from its nucleotide sequence, it can be modified and then "built" and characterized (Hellinga, 1997). If the protein structure is not available but its amino acid sequence displays a reasonable similarity with sequences of one or more proteins with known structure, through

homology modeling it is possible to predict its structure using as a template the structures of these homologous proteins. A simple example of this approach is the Swiss Model server (Schwed et al., 2003), a bioinformatics tool that allows to obtain protein structure models even if there isn't any molecular structure of the starting protein in any database. It performs an automated homology modeling once inserting the template structure and the multiple alignment of the protein of interest with the corresponding related proteins. As a result, the program provides a structural model and reiterating the process, in which theoretical and experimental approaches are alternated (the so-called "design cycle" Fig. 1), the user can refine the parameters to obtain the best molecular model of the desired protein (Stemmer and Holland, 2003). Computational biochemistry and recombinant DNA techniques give the best contribution to *rational design*. The considerable progress in computational biochemistry and the development of advanced algorithms allow to design the best molecular model to accommodate the desired protein changes which will be the one with lower energy conformation. In the meantime, the PCR-based site-specific mutagenesis is the most common technique used to introduce the desired mutations (deletions, insertions, substitutions) only in the specified gene, or even in a specific gene region. The mutated protein can be chemically synthesized or expressed in a recombinant system, such as *E. coli* or *P. pastoris*, and then analyzed for the modified function. In the latter case, the mutated protein is usually expressed in recombinant form fused to some tag protein or peptide, such as glutathione-S-transferase (Smith, 2000), thioredoxin (LaVallie et al., 2000), polyhistidine (Bornhorst and Falke, 2000) or maltose-binding protein (Chen and Gouaux, 1996), in order to make the protein purification easyer. An example of the great potential of the *rational design* strategy, is the huge amount of work on the serin-protease subtilisin, one of the first protein engineering model system since the early 1980's (Bryan, 2000). Since the subtilisin's structure was known, through a widespread rational mutagenesis on its amino acid sequence, during the years almost all its properties have been analyzed and modified to make this enzyme more active and more stable also in not-optimal conditions. It has been possible, for example, to make the subtilisin able to catalyze peptide ligase reaction, which normally doesn't occur in aqueous solution, allowing to synthesize peptides (Abrahmsen et al., 1991; Chen and Robinson, 1991). The rational design has important applications in enzymology, where the need for enzymes with best performances is growing. In fact, the most part of the enzymes commonly used in industrial processes are engineered through rational design to obtain thermal stability (Lin, 2008), a key role parameter

in using enzymes in biotechnological processes, to confer reaction product steroselectivity (Vallin et al., 2010) and activity in organic solvent (Castro and Knubovets, 2003). Protein rational design is also becoming an increasingly useful tool for optimizing protein drugs and creating novel biotherapeutics (Lazar et al., 2003). The great achievements over the years have broadened the horizons of *rational design* in the design of enzymes with functions that do not exist in nature, with potential applications in biotechnology, biomedicine and industrial processes.

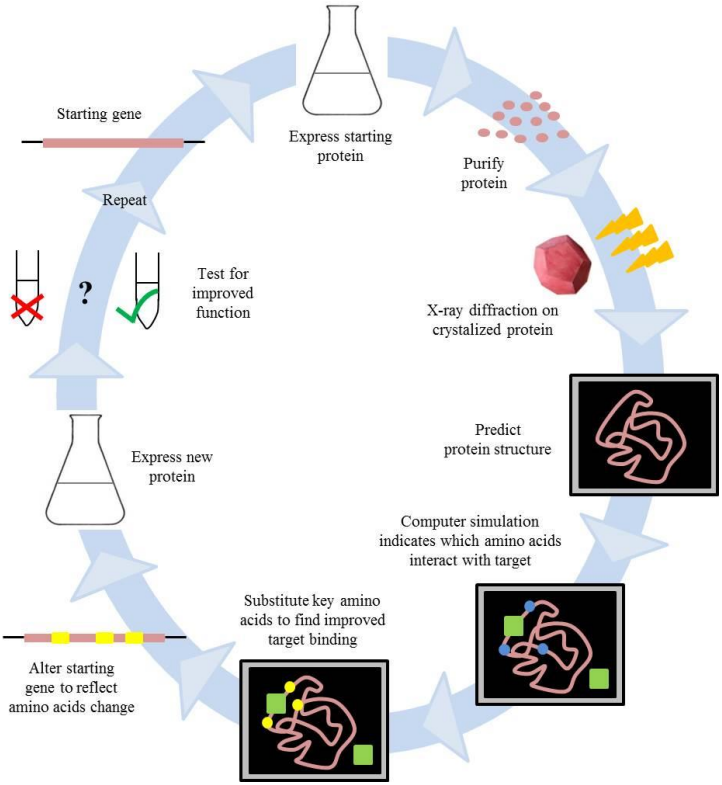

Figure 1. The *rational design* cycle. To optimize a known protein, the starting gene product is purified and crystallized. A computer model identifies key sites that interact with a target molecule. Based on an understanding of the physical principles that govern these interactions, specific amino acid changes can be tested that may improve protein function. (Adapted from Stemmer and Holland, 1994)

1.2 Directed evolution

The *directed evolution* strategy simulates the mechanisms that underlie biological evolution, *i.e.* the production of a large number of gene variants, the following selection of the most suitable protein variant and the amplification of their corresponding genes. Differently from the *in vivo* evolution, that needs thousands or even millions of years to generate new genes variants, *directed evolution* allows to obtain the same results in a much shorter timeframe. The main advantage of this strategy is that it only needs the gene sequence of the starting protein, without any additional structural information. The *directed evolution* involves an iterative strategy: once defined the target gene, a large library of mutants is generated by introducing random DNA mutations and finally, through a high-throughput screening, the best mutants are selected and used as starting point for a next cycle (Stemmer and Holland, 2003). The two natural evolutionary processes that have been adapted for *in vitro* evolution are random mutagenesis and gene recombination. The random mutagenesis is the first and the most simple system developed to generate molecular diversity. At the beginning were used chemical compounds or UV rays to introduce mutations (Botstein and Shortle, 1985), while currently the most commonly used system is the PCR-based mutagenesis. Another common protocol is the fragmentation of parental DNA into small nucleotide sequences and the following reconstitution of the entire gene through shuffling of such nucleotide fragments. This systems do not create predicted mutations at molecular level, but simply rearrange multiple existing sequences, allowing to obtain usually correctly folded and functional chimeric proteins, exploiting the variation naturally existing between them to generate new mutant genes with new sequences. The first homologous recombination-based system, named DNA shuffling, has been introduced by Stemmer in the early '90 (Stemmer, 1994). These recombinant strategies require parental sequences with a quite high homology degree, but sometimes it may be desirable to obtain completely new combinations shuffling non related genes (Table 1). The mutagenesis via non homologous recombination exploits the fact that many proteins, although showing a low degree of sequence homology have a similar three dimensional structure, thus increasing the possibility to obtain correctly folded chimeric proteins (Table 2). *Directed evolution* has been used with great success in recent years for optimization of enzymes' functional parameters by generation of new gene sequences, to improve their performances in defined operating conditions. Since the late 1990's *directed evolution* has been used to enhance enzyme properties such as

thermostability (Moore and Arnold, 1996; Suen et al., 2004; Diaz et al., 2011), tolerance to organic solvents (Song and Rhee, 2001) and pH profile (Bessler et al., 2003). Combining both the *rational design*, previously described, and the *directed evolution*, it has been possible to change stereo/enantio specificity (Zhang et al., 2000; Sacchi et al., 2004), and even to expand enzymes' substrate specificity (Bolt et al. 2008; Cheriyan et al., 2011).

Table 1. Homologous recombination methods

Methods	Advantages	Disadvantages	References
DNA shuffling	Flexible; back-crossing to parent removes non essential mutations.	Biased to crossing over in high homology regions; low crossingover rate; high percentage of parent.	Stemmer, 1994
RACHITT	No parental gene in a shuffling library; higher rate of recombinant; recombine genes of low sequence homology.	Complex; requires synthesis and fragmentation of single-strand complementary DNA.	Coco et al., 2001
StEP	Simplicity	Need high homology; low crossing over rate; needs tight control of PCR	Arnold et al., 1998

Table 2. Non-homologous recombination methods

Methods	Advantages	Disadvantages	Reference
Exon shuffling	Preserve exon function.	Requires known intron-exon organization of the target gene; limited diversity.	Kohlman and Stemmer, 2001
ITCHY	Eliminate recombinant bias; structural knowledge not needed.	Limited to two parents; significant fraction of progeny out-of-frame; complex labor-intensive.	Ostermeier et al.,1999
SHIPREC	Crossing overs occur at structurally related site.	Limited to two parents; single crossing over per gene.	Sieber et al., 2001

Table 1, ***table 2***: adapted from Rubin-Pitel et al., 2010

1.3 *De novo* design

The *de novo design* has been defined as the "Holy Grail" of protein engineering (Barrozo et al., 2012) because it makes possible to rapidly design effective biological proteins doing variations on known scaffold or completely from scratch. *De novo design* proved to be an interesting tool for protein structure-function studies and to exploit this knowledge to design proteins with completely new activities not existing in nature. To design a *de novo* protein or peptide one must take into account both the thermodynamic factors stabilizing the individual structural elements, as well as those that stabilize the entire structure. The starting thermodynamics hypothesis is that the native state of a protein is given by the amino acid sequence conformation that minimizes the structure energy. Algorithms, based on the physical properties that govern protein folding and stability, allow to find the best amino acid sequence fitting in a selected fold which will be associated with a specific function. Rosetta server (Liu and Kuhlman, 2006 - also available as standalone software) allows to obtain an *ab initio* protein structure prediction, using a semi-empirical force field for the evaluation of the predicted structure thermodynamics. Moreover, the server uses a Monte Carlo optimization algorithm for refining the simulation returned. Thanks to the considerable progress in the development of computational methods, towards the end of the 20th century it was possible the complete redesign of proteins starting from known scaffolds (Dahiyat and Mayo, 1997) and the development of novel protein fold (Burkhard et al., 2000; Kuhlman et al., 2003). Recently have been designed proteins with arbitrary three dimensional structure, removing the constraint of having scaffolds based on known protein backbones (MacDonald et al., 2010). This result was achieved designing an enzyme able of base-catalyzed benzisoxazole ring opening, also known as Kemp elimination (Röthlisberger, Baker et al., 2008. Fig. 2A), and stereoselective Diels-Alder reaction (Siegel et al., 2010. Fig. 2B). In both cases, the results obtained have considerable importance, since there are no enzymatic counterparts in nature catalyzing these reactions, widely used for chemical organic synthesis.

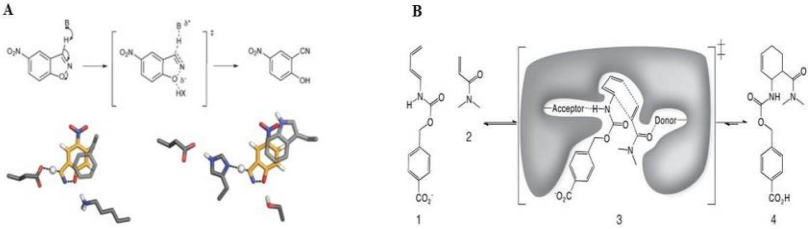

Figure 2. Reaction schemes and catalytic motifs used in design of the novel enzymes performing (A) Kemp elimination and (B) Diels-Alder reaction. In both the cases, was designed ex novo the enzyme's target active site, containing a pocket that ensuresthe substrates optimal orientation for catalysis. (Adapted from Siegel et al., 2010).

1.4 Scaffold for protein engineering

The idea of using stable protein structural motifs as scaffolds for reproducing functional epitopes or to stabilize bioactive conformations, is currently one of the most successful approaches of protein engineering (Razeghifard et al., 2007), in which converge both the *rational design* and the *directed evolution* as well as the *de novo design* strategies. It has been possible, in this way, to introduce new features in compatible known scaffolds, using the combinatorial protein design methods (Fig. 3A). Nature has always used common structural motifs and protein domains to accommodate different biological functions, the best example is certainly the immunoglobulin fold, in which a hypervariable sequence in the complementary region lies in a constant structure, giving rise to a huge number of different molecules. The immunoglobulin fold has been, in fact, one of the first stable scaffolds engineered to obtain new target specificity (Bruning et al., 2012). Other small natural scaffolds engineered to accommodate new functions are, for example, the α/β scorpion toxin fold (Vita et al., 1995) or B and Z domains of the Staphylococcal protein A (Wahlberg et al., 2003) (Fig. 3B). This protein engineering strategy allows to reproduce the functionality of an entire and complex protein in a small structural motif, and in this process the *rational approach* and the *de novo design* have given an important contribution, which have resulted in the development of miniproteins with new functions, introducing new binding sites in both existing and artificial scaffolds (Martin et al., 2000). The small size of such engineered miniproteins, makes easier their chemical synthesis

and the incorporation of tags and chemical modifications, useful for a wide range of applications. For example, starting from the staphylococcal protein A scaffold, binding proteins called "affibodies" have been engineered and extensively used in biochemistry (Nord et al, 2001), in diagnostic imaging (Orlova et al., 2006) and targeted therapy (Tolmachev et al., 2007) thanks to their Ig-mimic high binding specificity. The disulfide-rich peptides belonging to the knottin family are particularly interesting from this point of view, since they share an identical structural fold while having very different sequences and functions in plants, cone snails, and spiders (Norton and Pallaghy, 1998). The covalent bonds between the cysteine residues give the greatest contribution to the structure stability, allowing the variability of the remaining amino acid sequence. Among knottins, the highest tolerance to sequence variability is observed in conotoxins, neurotoxic peptides from cone snails venom, frequently cited as an example of natural combinatorial chemistry (Olivera, 2007). Conotoxins are characterized by multiple disulfide bridges and nature, during the evolution, has engineered this stable scaffold to express a great variety of neurotoxins with tuned specificity for different ion channels, both voltage-gated and ligand-gated, and receptors (Olivera and Teichert, 2007). As a result, their scaffold represents an excellent starting point for design strategies aimed at developing new miniproteins with new properties.

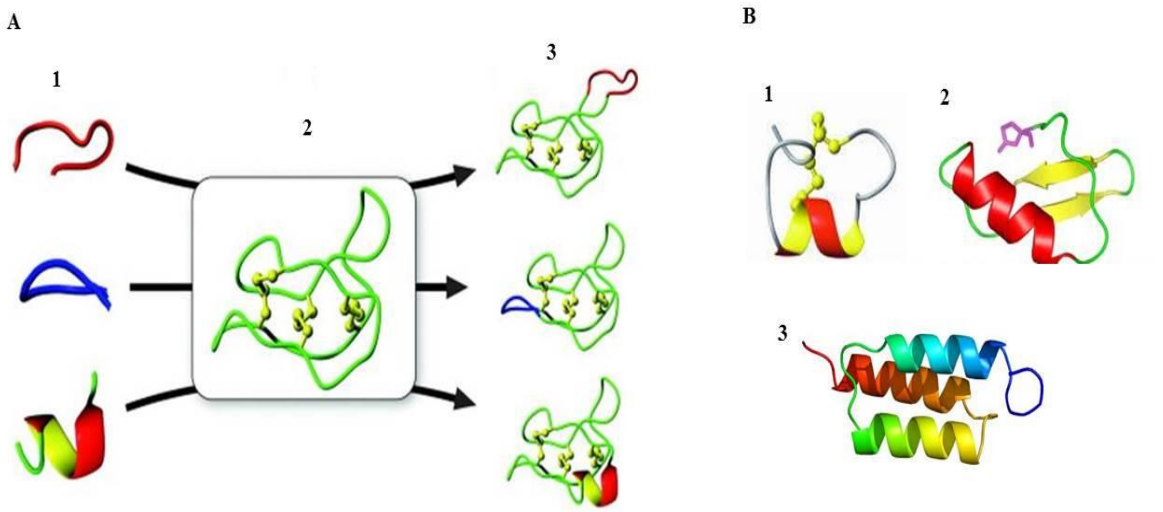

Figure 3. Strategy for the use of scaffolds in protein engineering. (A) An example of a peptide epitope grafting into a cyclic peptide scaffold. 1: Epitopes of different conformation, 2: Cyclic peptide used as scaffold, 3: Modified cyclic peptides, in which the epitopes are grafted into one of the native cyclic peptide loops. (B) Some common natural scaffold used to accomodate epitopes. 1: Conotoxin PnIA, 2: Charybdotoxin (scorpion toxin) and 3: Z domain of staphylococcal protein A (Adapted from Thorstholm and Craik, 2012).

1.5 Conotoxins

Conotoxins are bioactive peptides from the venom of mollusks of the genus *Conus*, widespread in tropical and subtropical marine environment (Fig. 4). Their venom is a complex mixture of different types of molecules that act in synergy to immobilize preys, and conotoxins represent the most abundant component in the venom (Olivera et al., 1991). All conotoxins are initially expressed as a large precursor peptide that undergo post-translational modification to yield the mature toxin, typically 10–40 amino acids long (Buczek et al., 2005). Even if the pre- and pro-region of precursor peptides result well conserved, the mature toxins are characterized by an high sequence variability, except for the cysteine residues. The most reliable theory about the evolutionary origins of this variability states that the intronic regions, flanking the mature toxins coding sequence, probably led to some recombination or replication events, as observed in the immunoglobulin loci. Conticello and coworkers (2001) studying conopeptide precursor alignments observed an accelerated rate of nucleotide substitution in the mature peptide region with respect to the pre- and pro-regions and a position-specific conservation of cysteine codons within the hypervariable region. To explain the evolutionary origin of conopeptide sequences hypervariability, they proposed a mutator mechanism targeted to mature domains in conopeptide genes, combining a protective activity specific for cysteine codons and a mutagenic polymerase that exhibits transversion bias (Conticello et al., 2001). About 500 cone snail species are known, and it has been estimated that there are about 100,000 different toxins, each one with particular pharmacologic properties (Terlau and Olivera, 2004). Despite their large number, all conotoxins are produced by translating mRNA from genes belonging to only sixteen superfamilies (Kaas et al., 2010) divided according to the relative conservation of the signal peptide. They are also divided in groups based on the cysteine framework, and in pharmacological families based on their molecular target. Because of their high potency and target specificity, conotoxins have attracted much interest as tools for investigating ion channels function, as neuropharmacological tools, as potential leads in drugs development, or indeed as drugs themselves (Adams et al., 1998). Currently the ω-conotoxin MVIIA from *Conus magus* is used as analgesic drug in its synthetic analogue Ziconotide (Wermeling, 2005). Generally, candidate molecules to be used as scaffold for protein engineering should have a structure characterized by a flexible external surface able to withstand sequence hypermutation without interfering with the core folding. They should be

small and soluble monomeric polypeptides with a stable structure, easily to engineer and efficiently produce with high yield in expression systems (Nord et al., 1997). Conotoxins satisfy all these parameters and in addition have a remarkable high target specificity that make them excellent models for redesign strategies aimed to generate both more stable and active conotoxins for therapeutics (Clark et al., 2005), and to engineer miniproteins with novel functions. From the natural source, the purification of conotoxins is very difficult because of the large number of specimens needed to obtain a sufficient amount of venom to process. Moreover, as previously said, the venom is a mixture of hundreds of different molecules, each one present in very small amount. To overcome this problem, two approaches are available: chemical synthesis and recombinant expression in heterologous systems. The chemical synthesis has been the method of choice, because conotoxins share the characteristic of being extensively post translational modified (Buczek, 2005). However, this procedure is quite expensive. The use of recombinant expression systems, both prokaryotic and eukaryotic cells, is the cheapest choice, and allows to obtain peptides in large quantities, as well. The major drawback is the limited post translational machinery that does not permit the production of peptides with the kind of post translational modifications observed in most conotoxins. Small peptides such as conotoxins usually are difficult to express in the *E.coli* system, because they are quickly degraded by cellular proteases or aggregate in the inclusion bodies. Moreover sometimes the overexpression of heterologous proteins is toxic for bacteria. For this reason, to obtain a high yield of soluble small proteins, the best successful strategy is to express them in fusion with carrier proteins, such as maltose-binding protein (Kapust and Waugh, 1999), thioredoxin (LaVallie et al., 2000), or glutathione S-transferase (Nygren et al., 1994). This carrier acts also as a tag to easily purify the recombinant protein by affinity chromatography.

Figure 4. Shells of some mollusk-hunting *Conus* species. Top row (left to right): *C. ammiralis, C. aulicus, C. bandanus and C. crocatus*. Middle row (left to right): *C. dalii, C. episcopatus, C. furvus, C. gloriamaris*. Bottom row (left to right): *C. immelmani, C., marmoreus, C. omaria, C. textile* (From Nam et al., 2009).

1.6 Aim of the work – Development of an expression system for natural and redesigned disulphide-rich peptides

A system has been developed to express in *E. coli* cells disulfide-rich miniproteins in recombinant form, as GST fusion proteins. As a test case, the new protocol has been used to express the conotoxin Vn2 (wt CTX) from the Mediterranean Sea *Conus ventricosus*, a 33 amino acids long highly hydrophobic neuropeptide, and the Asp2His CTX Vn2 mutant (mt CTX) (Spiezia et al., 2012). The worm-hunting *C. ventricosus* has an array of toxins that synergically act on invertebrate ion channels and receptors to immobilize the prey. Thus, to assess if the expression system developed allows to obtain disulphide-rich peptides correctly folded and active, the bioactivity of both recombinant CTXs has been assayed in a toxicity test using the larvae of the moth *Galleria mellonella*, a well know invertebrate model system (Spiezia et al., 2012). Further, to test the potential of conotoxins natural scaffold for rational design applications, another conotoxin, ω-conotoxin GVIA, has been used as a starting point to develop a copper binding minimetalloprotein, with the aim to generate a novel biocatalyst (Barba et al., 2012). Through computational modeling, two disulphide bridges have been replaced with His residues and the redesigned peptides, named Cupricyclin-1 and Cupricyclin-2, have been synthesized

and characterized for their copper binding ability and superoxide dismutase activity (Barba et al., 2012).

1.7 Work in progress

The synthetic peptides Cupricyclin-1 and -2, redesigned starting from the ω-conotoxin GVIA, bind copper ions with a fairly high affinity, and display a superoxide dismutase activity comparable to other superoxide dismutase mimics (Riley, 1999). These good results have represented the starting point to improve the catalytic performance of the redesigned minimetalloproteins by generating novel variants with different metal-binding specificity. The high catalytic efficiency of SODs is due to their peculiar electrostatic potential distribution on the protein surface. In particular, in Cu, Zn SODs the positively charged catalytic site lies in a negatively charged environment, making productive any collision of the substrate with SOD molecules via electrostatic steering effect (Desideri et al., 1992). Starting from this assumption, a Cupricyclin-1 mutant K27E/R28E has been generated. The Lys27 and Arg28 are located on the opposite side of the copper accessible site, for this reason they have been replaced with negatively charged amino acids to mimic the SOD surface charge asymmetry. While Cu, Zn SODs rely on a bimetallic cluster to carry out superoxide dismutation it is well known that also mononuclear metal centers based on iron, manganese and nickel display superoxide dismutase activity. In Mn and Fe SODs, in particular, the metal ion is coordinated by one Asp and three His residues (Miller, 2004). Since Cupricyclin-1 binding site is formed by 4 His, an iron- or manganese-binding site has been introduced in this peptide by replacing His29 with an Asp, obtaining the H29D mutant. The additional triple mutant K27E/R28E/H29D was also generated which is expected to have increased SOD activity and Fe and Mn ions binding specificity.
The interest in these redesign strategies derives also from the possibility of using minimetalloproteins as biosensors for the detection of metals. A variety of non-enzymatic proteins, ranging from naturally occurring metal-binding proteins to engineered proteins binding specific metal ions, are currently used in biosensor development (Tien et al., 2002; Verma and Singh, 2005). Given the properties and activity of the redesigned Cupricyclin-1 and -2 and potentially of the novel mutants, these minimetalloproteins could be used both for detection of the amount of

heavy metals and the determination of O_2^- radicals. The ability to dismutate superoxide anions could open the possibility to use these novel minimetalloproteins also as therapeutics in oxidative stress injuries. In fact, excessive reactive oxygen species (ROS) lead to some important neural disorders such as Alzheimer's and Parkinson's disease (Emerit et al., 2004) or epilepsy (Azam et al., 2012), as well as cardiovascular diseases like hypertension and atherosclerosis (Griendling and Fitzgerald, 2003).

2. RESULTS AND DISCUSSION

2.1 Articles published

The most part of the results achieved during my Ph.D. thesis are published in the following articles reported in the Supplementary Material section.

- Spiezia, M.C., Chiarabelli, C., Polticelli, F. (2012). Recombinant expression and insecticidal properties of a Conus ventricosus conotoxin-GST fusion protein. *Toxicon*, 60:744-751
- Barba, M., Sobolev, A.P., Zobnina, V., Bonaccorsi di Patti, M.C., Cervoni, L., Spiezia, M.C., Schininà, M.E., Pietraforte, D., Mannina, L., Musci, G., Polticelli, F. (2012). Cupricyclins, Novel Redox-Active Metallopeptides Based on Conotoxins Scaffold. *PLoS ONE*, 7(2):e30739

2.2 Construction of the expression vector

To obtain the GST-fusion proteins, Cupricylin-1 mutant 1 (H29D), mutant 2 (K27E/R28E) and mutant 3 (K27E/R28E/H29D) nucleotide sequences were amplified by PCR, using as template the sequence CPK wt (see materials and methods section), and then cloned into the pET42b plasmid, cutting the plasmid and the amplified sequences with SacII and BamHI restriction enzymes. Some technical expedients were used to avoid problems during the cloning and expression protocols. In detail, the forward primer for the cloning of Cupricyclins nucleotide sequences in the pET42b plasmid (FW CPK1_pET42b, see Fig. 2 in materials and methods section) was designed to contain upstream SacII recognition site plus 6 additional nucleotides required for an optimal digestion of the endonuclease, and a nucleotide sequence coding for the tripeptide Gly-Ser-Arg, to be placed immediately upstream the Cupricyclins (CPCs) coding sequences, avoiding the possibility of uncorrected folding of the recombinant proteins. In fact this tripeptide spacer is expected to reduce the steric hindrance between GST and the first Cys residue of CPCs sequence, involved in a disulphide bridge formation (Fig. 5). Moreover, the Gly residue of the tripeptide forms part of

a thrombin recognition site (Pro-Arg-Gly) useful for the cleavage of the GST tag during CPCs purification. The reverse primers (RV CPK H29D, RV CPK K27E_R28E and RV CPK K27E_R28E_H29D, see Fig. 2 in materials and methods section), used to introduce the mutations in the wild-type Cupricyclin-1 nucleotide sequence, also contains plus 6 additional nucleotides downstream BamHI site for an optimal digestion. Finally, a stop codon optimized for expression in *E. coli* system was introduced at the end of CPCs sequences. To test the expression system developed, the wild-type Cupricyclin-1 (wt CPC) has been expressed as a GST-fusion product.

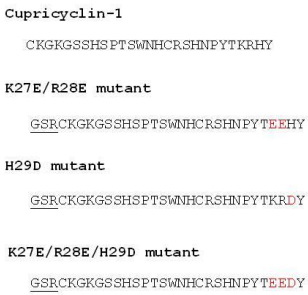

Figure 5: The amino acid sequences of Cupricyclin-1 redesigned peptide (wt CPC) and the three mutants. The mutated residues are in red, the tripeptide inserted upstream the amino acid sequence is underlined.

2.3 Recombinant proteins expression and purification

The expression and purification protocols were the same used for wild-type and Asp2His GST-conotoxins (For detail, see *Results* section in Spiezia et al., 2012). The experimental procedures have allowed to obtain, also in this case, high yield in purified recombinant GST-CPCs (Fig. 6).

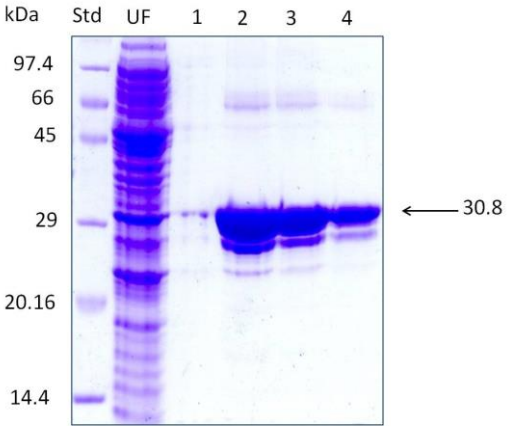

Figure 6. 12% SDS PAGE analysis of purified GST-CPC mutant 1 (H29D) by GST-affinity chromatography. Std: Protein SHARPMASS Low (*Euroclone*) marker; UF: unbound fraction; lane 1-4: eluted fractions. All the recombinant wt CPC and CPC mutants gave the same electrophoretic pattern.

2.3.1 Isolation of the recombinant Cupricyclins

The purified GST-CPCs proteins were dialyzed against Tris-HCl 20 mM, pH 8.0 and then digested overnight with thrombin, to remove the GST tag. Exploiting the high thermostability reported for the synthetized Cupricyclin-1 (Barba et al., 2012), heat treatment of the digested samples first at 55°C and then at 90°C was performed to separate the GST tag from the peptides. After heating the samples, in fact, only the CPCs were present in the soluble fraction, while the GST tag precipitated, as revealed by the 12% SDS-PAGE analysis (Fig. 7).

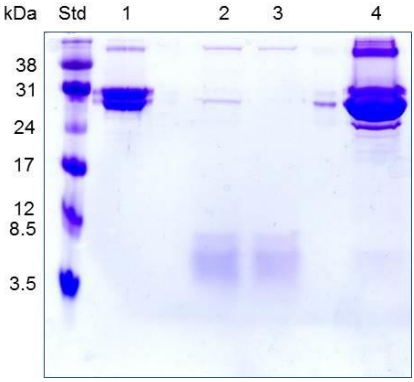

Figure 7. 12% SDS PAGE analysis of CPC mutant 1 before and after thrombin and heat treatments. Std: Rainbow marker Low Range (*GE Healthcare*); lane 1: CPC mutant 1 before cleavage (MW 30.8 kDa); lane 2: supernatant after 55°C treatment; lane 3: supernatant after 90°C treatment; lane 4: 90°C pellet. The same pattern was observed for wt CPC and CPC mutants 2 and 3.

2.4 Mass spectrometry characterization of recombinant CPCs

Mass spectrometry analyses were carried out in order to uniquely identify the wt CPC and CPC mutants isolated from the GST tag by thrombin cleavage and heating treatments. Each sample was treated with iodoacetamide (IAM), an alkylating agent that interacts with cysteine residues, digested with trypsin and then analyzed by MALDI TOF. As expected, the MALDI TOF spectra revealed two main peaks for each Cupricyclin, one of them, with an observed molecular weight of about 1512.64 Da, common to all the peptides. Its molecular weight was higher than the theoretical value, calculated with PeptideMass tool (from ExPASy bioinformatics resource portal), of about 57 Da. This difference was consistent with the carboxyamidomethylation of Cys19 residue by IAM (Tab. 3). The molecular weight of the second peaks in CPC mutant 2 and 3 mass spectra were different compared to wt CPC and CPC mutant 1, since the K27E mutation abolishes the Lys27 recognition site for trypsin.

Cupricyclin	Theoretical fragments mass (Da)	Observed fragments mass (Da)	Sequence
Wild type	F1: 1455.62 F2: 846.41	F1:1520.71 F2: 847.19	GSRCKGK|GSSHSPTSWNHCR|SHNPYTK|RDY F1 F2
Mutant 1	F1: 1455.62 F2: 846.41	F1:1522.69 F2: 849.69	GSRCKGK|GSSHSPTSWNHCR|SHNPYTK|RHY F1 F2
Mutant 2	F1: 1455.62 F2: 1276.52	F1: 1517.06 F2: 1251.09	GSRCKGK|GSSHSPTSWNHCR|SHNPYTEEHY F1 F2
Mutant 3	F1: 1455.62 F2: 1254.49	F1:1519.10 F2:1241.41	GSRCKGK|GSSHSPTSWNHCR|SHNPYTEEDY F1 F2

Table 3. Mass spectrometry analysis summary on wt CPC and CPC mutants. The difference in the observed F1 fragment molecular weight, compared with the theoretical one, is due to the Cys19 alkylation by IAM. Arrows indicate the trypsin cleavage sites that generate the two main peaks observed in MALDI TOF spectra for each Cupricyclin. The amino acid substitution in the CPC mutants are in red and the cysteine residues alkylated are underlined.

2.5 Preliminary data on Cupricyclins metal binding ability

2.5.1 Recombinant expression system validation

Evidence of Cu^{2+} binding to wt CPC expressed in *E. coli* was first obtained by fluorescence quenching experiments, exploiting the ability of copper ions to quench the fluorescence emitted by the single Trp16 upon binding to the miniprotein. Fluorescence quenching was dependent on metal concentration and reached a maximum at a $[Cu^{2+}]$/[peptide] of approx. 1:1 ratio. A non linear regression curve fitting of the fluorescence intensity decrease as a function of Cu^{2+} concentration gave a copper dissociation constant K_D of 1.77 (±0.3) x 10^{-7} M (Fig. 8), the same order of magnitude reported for the chemically synthetized Cupricyclin-1. Further evidence of copper-wt CPC binding was obtained by optical spectroscopy analysis. Addition of a stoichiometric amount of $CuCl_2$ to the peptide (0.6 μM final concentration) induced the appearance of an absorption band at approx. 700 nm (Fig. 9), typical of copper complex with His ligands. These results have confirmed the validity of the recombinant expression system developed for the expression of disulphide-rich minimetalloproteins.

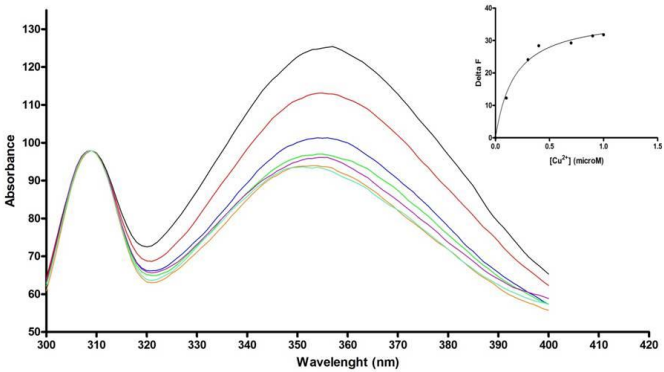

Figure 8. Emission fluorescence spectra of wt CPC in the presence of increasing amounts of Cu^{2+} ions. Black line: apo wt CPC (0.6 μM); red line: apo+$CuCl_2$ 0.1 μM; blue line: apo+$CuCl_2$ 0.3 μM; green line: apo+$CuCl_2$ 0.4 μM; violet line: apo+$CuCl_2$ 0.7 μM; orange line: apo+$CuCl_2$ 0.9 μM; light blue line: apo+$CuCl_2$ 1 μM. **Inset**: Determination of the dissociation constant of Cu^{2+} to wt CPC by fluorescence quenching experiments. The non linear fitting curve of fluorescence decrease at 352 nm as function of increasing amounts of Cu^{2+} ions is shown as a continuous line.

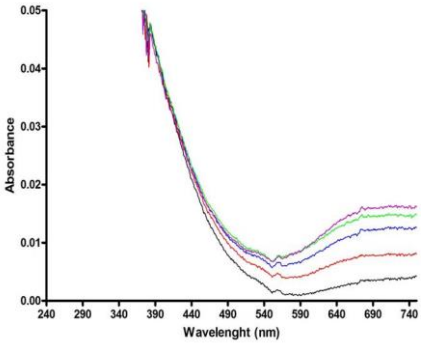

Figure 9. Optical spectra of wt CPC (0.13 mM in Tris-HCl 20 mM, pH 8.0) in the presence of increasing amounts of Cu^{2+} ions. Black line: apo wt CPC; red line: 0.25:1 [Cu^{2+}]/[peptide] ratio; blue line: 0.5:1 ratio; green line: 0.75:1 ratio; violet line: stoichiometric ratio 1:1.

2.5.2 Characterization of the novel metallopeptides

The metal binding properties of CPC mutants, designed to bind iron and manganese instead of copper (mutants 1 and 3), or to bind copper ions with an increased SOD activity as compared with wt CPC (mutant 2), were analyzed by optical spectroscopy. Aliquots of $FeCl_3$, $MnCl_2$ (mutants 1 and 3) and $CuCl_2$ (mutant 2) were added to the samples and spectra were recorded between 240 nm and 750 nm. Both mutants 1 and 3 did not display any significant affinity for Mn^{2+} ions, and only a low affinity for Fe^{3+}, since saturation of the optical signal in this latter case was observed only for high [metal]/[peptide] ratio (Fig. 10). Surprisingly, mutant 2 showed no copper binding ability. However once analyzed for Fe^{3+} binding, a significant difference in absorption spectra with increasing $FeCl_3$ concentration was observed, reaching the maximum at the stoichiometric ratio [Fe^{3+}]/[peptide] 1:1. The difference spectrum showed a clear band at 300 nm and minor bands at 420 and 460 nm (Fig. 11).

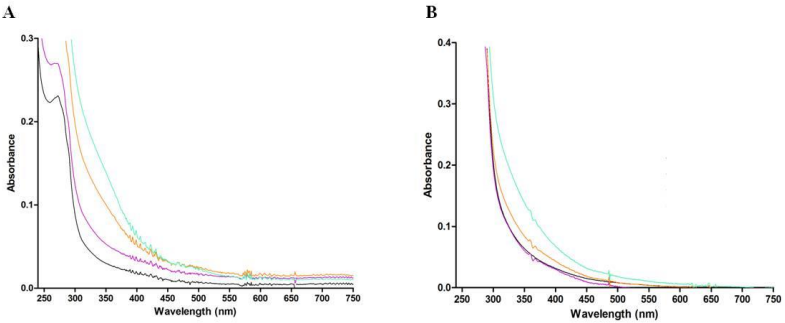

Figure 10. Optical spectra of (A) CPC mutant 1 and (B) mutant 3 (2.8 x 10^{-5} M and 5.8 x 10^{-5} M, respectively, in Tris-HCl 20 mM pH 8.0) in the presence of increasing concentrations of Fe^{3+} ions. Black line: apo peptides; violet line: stoichiometric [Fe^{3+}]/[peptide] 1:1 ratio; orange line: 2:1 ratio; light blue line: 5:1 ratio.

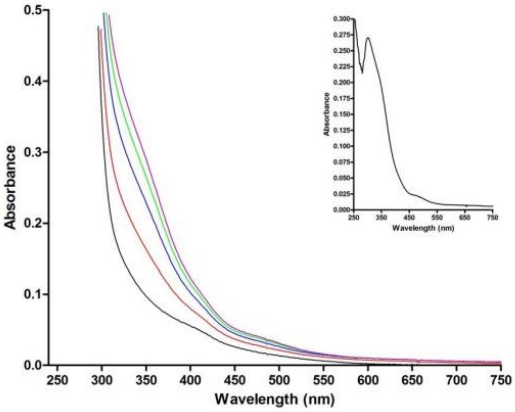

Figure 11. Optical spectra of CPC mutant 2 (in Tris-HCl 20 mM pH 8.0) in the presence of increasing amounts of Fe^{3+} ions. Black line: apo peptide; red line: [Fe^{3+}]/[peptide] 0.25:1 ratio; blue line: 0.5:1 ratio; green line: 0.75:1 ratio; violet line: stoichiometric ratio 1:1. **Inset**: Difference spectrum between holo and apo CPC mutant 2 to evidence the appearance of a band at 300 nm.

Despite the encouraging results obtained on the CPC mutant 2, the experimental protocols conducted so far don't allow to collect enough detailed data to characterize its redox activity. Currently, a large scale production of this peptide is in progress in order to obtain higher quantities of this peptide.

3. CONCLUSION AND PERSPECTIVES

The work described so far is part of a larger project aimed to investigate the potential biotechnological application of conotoxins, disulphide-rich neuropeptides from cone snail venom. Two of their peculiar properties, the high target specificity and the tolerance to sequence hypervariability, have been explored. My doctoral thesis work can be divided in three parts.

- Development of an expression system for overproduction of the Conotoxin Vn2 from *C. ventricosus*, its functional characterization and potential application for the development of environmental-friendly pesticides. This expression system has allowed the expression of Conotoxins Vn2, and its Asp2His mutant, as GST fusion proteins and the obtainment of a high yield in soluble and active peptides. Neurotoxic activity assays of these recombinant proteins in an insect model system evidenced a high GST-conotoxins toxicity at a concentration of only few tens of pmol/g of body weight (Spiezia et al., 2012).
- The design and synthesis of novel copper-binding peptides, named Cupricyclin-1 and -2, based on the well characterized ω-conotoxin GVIA scaffold. In these novel metallopeptides a four His cluster was introduced in the place of four of the six Cys residues in the original sequence, generating a copper-binding site in the same disulphide constrained structure. Both the peptides showed a superoxide dismutase activity comparable with other SOD-mimics, opening up the possibility to use Cupricyclin-1 and -2 as catalysts in antioxidant reactions and bioremediation (Barba et al., 2012).
- The application of the high-yield expression system developed, for overproduction of GST-Cupricyclin-1 (CPC) mutants, designed with the aim to introduce different metal specificity and increase CPCs SOD activity. Preliminary data on the expressed wild-type CPCs has confirmed the validity of the system developed. In fact the recombinant peptide displays a copper affinity and spectroscopic properties very similar to those of the corresponding synthetic peptide. Characterization of the CPC mutants has revealed some unexpected but interesting results.

In particular, the CPC mutant 2 (K27E/R28E) proved to be the most promising for further development. In fact, at variance with the other two mutants, this peptide displays a good iron binding ability. Large scale production of this peptide is needed in order to characterize its redox properties. Once a complete characterization of CPC mutant 2 properties will be carried out, an interesting perspective could be to explore its

potential as an antioxidant molecule for the treatments of oxidative stress injuries. In fact, it is known that the balance between superoxide anions, one of the main reactive oxygen species (ROS) within cells, and antioxidants such as SODs, is a crucial factor in determining the onset of some important neurodegenerative diseases. To this aim, the CPC mutant 2 will be tested for its ability in preventing the increase of ROS concentration, using as a model glial and neuronal cells treated with glutathione oxidizing agents and electron transfer chain's inhibitors.

4. REFERENCES

Abrahmsen, L., Tom, J., Burner, J., Butcher, K.A., Kossiakoff, A., Wells, J.A. (1991). Engineering subtilisin and its substrates for efficient ligation of peptide bonds in aqueous solution. *Biochemistry*, 30(17):4151-4159.

Adams, D.J., Alewood, P.F., Craik, D.J., Drinkwater, R.D., Lewis, R.J., (1999). Conotoxins and their potential pharmaceutical applications. *Drug Develop Res*, 46:219–234.

Azam, F., Prasad, M.V., Thangavel, N. (2012). Targeting oxidative stress component in the therapeutics of epilepsy. *Curr Top Med Chem*. 12(9):994-1007.

Baker, D. (2006). Prediction and design of macromolecular structures and interactions. *Philos Trans R Soc Lond B Biol Sci*. 361(1467):459-63.

Barba, M., Sobolev, A.P., Zobnina, V., Bonaccorsi di Patti, M.C., Cervoni, L., Spiezia, M.C., Schininà, M.E., Pietraforte, D., Mannina, L., Musci, G., Polticelli, F. (2012). Cupricyclins, Novel Redox-Active Metallopeptides Based on Conotoxins Scaffold. *PLoS ONE*, 7(2):e30739.

Barrozo, A., Borstnar, R., Marloie, G., Kamerlin, S.C.L. (2012). Computational Protein Engineering: Bridging the Gap between Rational Design and Laboratory Evolution. *Inter J Mol Sci*, 13(10):12428-12460.

Bessler, C., Schmitt, J., Mauer, K.H., Schmid, R.D. (2003). Directed evolution of a bacterial α-amylase toward enhanced pH-performance and high specific activity. *Protein Sci*, 12(10):2141-2149.

Bolt, A., Berry, A., Nelson, A., (2008). Directed evolution of aldolases for exploitation in synthetic organic chemistry. *Arch Biochem Biophys*, 474(2):318-330.

Bornhorst, J.A., Falke, J.J. (2000). Purification of proteins using polyhistidine affinity tags. *Methods in enzymology*, 326:245-254.

Botstein, D., Shortle, D. (1985). Strategies and applications of in vitro mutagenesis. *Science*, 229(4719):1193-1201.

Bruning, M., Barsukov, I., Franke, B., Barbieri, S., Volk, M., Leopoldseder, S., Ucurum, Z., Mayans, O. (2012). The intracellular Ig fold: a robust protein scaffold for the engineering of molecular recognition. *Protein Eng Des Sel*. 25(5):205-12.

Bryan, P.M. (2000). Protein engineering of subtilisin. *Biochim Biophys Acta*, 29;1543(2):203-222. Review.

Buczek, O., Bulaj, G., Olivera, B.M., 2005. Conotoxins and the posttranslational modification of secreted gene products. *Cell Mol Life Sci*, 62:3067–3079.

Burkhard, P., Meier, M., Lustig, A. (2000). Design of a minimal protein oligomerization domain, a structural approach. *Protein Science*, 9(12):2294-2301.

Castro, G.R., Knubovets, T. (2003). Homogeneous biocatalysis in organic solvents and water-organic mixtures. *Crit Rev Biotechnol*, 23(3):195-231.

Cao, B., Nagarajan, K., Loh, K.C. (2009). Biodegradation of aromatic compounds: current status and opportunities for biomolecular approaches. *Appl Microbiol and Biotechnol*, 85(2):207-228.

Chen, K.Q., Robinson, A.C., Van Dam, M.E., Martinez, P., Economou, C., Arnold, F.H. (1991). Enzyme engineering for nonaqueous solvents. II. Additive effects of mutations on the stability and activity of subtilisin E in polar organic media. *Biotech Prog* 7(2):125-129.

Chen, G.Q., Gouaux, J.E. (1996). Overexpression of bacterio-opsin in *Escherichia coli* as a water-soluble fusion to maltose binding protein: Efficient regeneration of the fusion protein and selective cleavage with trypsin. *Prot Sci*, 5(3):456-467.

Cheriyan, M., Walters, M.J., Kang, B.D., Anzaldi, L.L., Toone, E.J., Fierke, C.A. (2011). Directed evolution of a pyruvate aldolase to recognize a long chain acyl substrate. *Bioorg Med Chem*, 19(21):6447-6453.

Chow, D., Nunalee, M.L., Lim, D.W., Simnick, A.J., Chilkoti, A. (2008). Peptide-based biopolymers in biomedicine and biotechnology. *Mat Sci Eng R Rep*, 62(4):125-155.

Clark, R.J., Fischer, H., Dempster, L., Daly, N.L., Rosengren, K.J., Nevin, S.T., Meunier, F.A., Adams, D.J., Craik, D.J. (2005). Engineering stable peptide toxins by means of backbone cyclization: Stabilization of the α-conotoxinMII. *Proc Natl Acad Sci USA*, 102(39):13767–13772.

Conticello, S.G., Gilad, Y., Avidan, N., Ben-Asher E., Levi, Z., Fainzilber, M. (2001). Mechanisms for evolving hypervariability: the case of conopeptides. *Mol Biol Evol*, 18:120-131.

Coco, W.M., Levinson, W.E., Crist, M.J., Hektor, H.J., Darzins, A., Pienkos, P.T., Squires, C.H., Monticello, D.J. (2001). DNA shuffling method for generating highly recombined genes and evolved enzymes. *Nature Biotechnology*, 19:354–359.

Dahiyat, B.I., Mayo, S.L. (1997). De Novo Design: Fully Automated Sequence Selection. *Scienc*e, 278(5335):82-87.

Desideri, A., Falconi, M., Polticelli, F., Bolognesi, M., Djinovic, K., Rotilio, G. (1992). Evolutionary conservativeness of electric field in the Cu,Zn superoxide dismutase active site. Evidence for co-ordinated mutation of charged amino acid residues. *J Mol Biol*, 223:337–342.

Diaz, J.E., Lin, C.S., Kunishiro, K., Feld, B.K., Avrantinis, S.K., Bronso, J., Greaves, J., Saven, J.G., Weiss, G.A. (2011). Computational design and selections for an engineered, thermostable terpene synthase. *Prot Sci*, 20(9):1597-1606.

Emerit, J., Edeas, M., Bricaire, F. (2004). Neurodegenerative diseases and oxidative stress. *Biomed Pharmacother*. 58(1):39-46. Review.

Griendling, K.K. and Fitzgerald, G.A. (2003). Oxidative stress and cardiovascular injury. Part I. Basic mechanisms and in vivo monitoring of ROS. *Circulation* 108:1912–1916.

Hellinga, H.W. (1997). Rational protein design: Combining theory and experiment. *Proc Natl Acad Sci USA*, 16; 94(19):10015-10017.

Kaas, Q., Westermann, J.C., Craik, D.J., 2010. Conopeptide characterization and classifications: an analysis using ConoServer. *Toxicon*, 55:1491–1509.

Kapust, R.B., Waugh, D.S. (1999). Escherichia coli maltose-binding protein is uncommonly effective at promoting the solubility of polypeptides to which it is fused. *Protein Sci*, 8:1668–1674.

Kolkman, J.A. and Stemmer, W.P.C. (2001). Directed evolution of proteins by exon shuffling. *Nature Biotech*, 19:423-428.

Kuhlman, B., Dantas, G., Ireton, G.C., Varani, G., Stoddard, B.L., Baker, D. (2003). Design of a Novel Globular Protein Fold with Atomic-Level Accuracy. *Science*, 302:1364-1368.

LaVallie, E.R., Lu, Z.J., Diblasio-Smith, E.A., Collins-Racie, L.A., McCoy, J.M. (2000). Thioredoxin as a fusion partner for production of soluble recombinant proteins in *Escherichia coli*. *Methods Enzymol*, 326:322-340.

Lazar, G.A., Marshall, S.A., Plecs, J.J., Mayo, S.L., Desjarlais, J.R. (2003). Designing proteins for therapeutic applications. *Curr Opin Struct Biol*, 13(4):513-518.

Lin, Y.S. (2008). Using a strategy based on the concept of convergent evolution to identify residue substitutions responsible for thermal adaptation. *Proteins*, 73(1):53-62.

Liu, Y., Kuhlman, B. (2006). RosettaDesign server for protein design. *Nucleic Acids Res*, 1; 34(Web Server issue):W235–W238.

MacDonald, J.T., Maksimiak, K., Sadowski, M.I., Taylor, W.R. (2010). De novo backbone scaffolds for protein design. *Proteins*, 78(5):1311-25.

Marklund, S., Marklund, G. (1974). Involvement of the superoxide anion radical in the autoxidation of pyrogallol and a convenient assay for superoxide dismutase. *Eur J Biochem* 47:469–474.

Martin, L., Barthe, P., Combes, O., Roumestand, C., Vita, C. (2000). Engineering Novel Bioactive Mini-Proteins on Natural Scaffolds. *Tetrahedron*, 56:9541-9460.

Miller, A.F. (2004). Superoxide dismutases: active sites that save, but a protein that kills. *Curr Opin Chem Biol*, 8:162–168.

Moore, J.C., Arnold, F.H. (1996). Directed evolution of a para-nitrobenzyl esterase for aqueous-organic solvents. *Nat Biotechnol*, 14(4):458-467.

Nam, H.H., Corneli, P.S.,Watkins, M., Olivera, B., Bandyopadhyay, P. (2009). Multiple genes elucidate the evolution of venomous snail-hunting Conus species. *Mol Phyl Evol*, 53(3):645-652.

Nygren, P.A., Stahl, S., Uhlen, M. (1994). Engineering proteins to facilitate bioprocessing. *Trends Biotechnol*, 12:184–188.

Nord, K., Nord, O., Uhlén, M., Kelley, B., Ljungqvist, C., Nygren, P.A. (2001). Recombinant human factor VIII-specific affinity ligands selected from phage-displayed combinatorial libraries of protein A. *Eur J Biochem*, 268(15):1–10.

Norton, R.S., Pallaghy, P.K. (1998). The cystine knot structure of ion channel toxins and related polypeptides. *Toxicon*, 36(11):1573-83.

Olivera, B.M., Rivier, J., Scott, J.K., Hillyard, D.R., Cruz, L.J., 1991. Conotoxins. *J.Biol Chem*, 266,2067–22070.

Olivera, B.M., Teichert, R.W. (2007). Diversity of the neurotoxic Conus peptides: a model for concerted pharmacological discovery. *Mol Interv*, 7:251–260.

Orlova, A., Magnusson, M., Eriksson, T.L., Nilsson, M., Larsson, B., Höidén-Guthenberg, I., Widström, C., Carlsson, J. (2006). Tumor imaging using a picomolar affinity HER2 binding affibody molecule. *Cancer Res*, 66 (8):4339–48.

Ostermeier, M., Shin, J.H., Benkovic S.J. (1999). A combinatorial approach to hybrid enzyme independent of DNA homology. *Nature Biotech*, 17:1205-1209.

Razeghifard, R., Wallace, B.B., Pace, R.J., Wydrzynski, T. (2007). Creating functional artificial proteins. *Curr Prot Pept Sci*, 8(1):3-18.

Riley, D.P. (1999). Functional Mimics of Superoxide Dismutase Enzymes as Therapeutic Agents. *Chem Rev*, 99:2573–2587.

Röthlisberger, D., Khersonsky, O., Wollacott, A.M., Jiang, L., DeChancie, J., Betker, J., Gallaher J.L., Althoff, E.A., Zanghellini, A., Dym, O., Albeck, S., Houk, K.N., Tawfik, D.S., Baker, D. (2008). Kemp elimination catalysts by computational enzyme design. *Science*, 453(7192):190-195.

Rubin-Pitel, S., Luo, Y., Lee, J.K., Zhao, H. (2010). A Diverse Family of Type III Polyketide Synthases in Eucalyptus Species. *Molecular Biosystems*, 6:1444-1446.

Sacchi, S., Rosini, E., Molla, G., Pilone, M.S., Pollegioni, L. (2004). Modulating D-amino acid oxidase substrate specificity: production of an enzyme for analytical determination of all D-amino acids by directed evolution Protein engineering. *Design & Selection*, 17:517-525.

Schwed, T., Kopp, J., Guex, N., Peitsch, M.C. (2003). SWISS-MODEL: an automated protein homology-modeling server. *Nucleic Acids Res*, 31:3381-3385.

Sieber, V., Martinez, C.A., Arnold, F.H. (2001). Libraries of hybrid proteins from distantly related sequences. *Nature Biotech*, 19:456-460.

Siegel, J.B., Zanghellini, A., Lovick, H.M., Kiss, G., Lambert, A.R., St Clair, J.L., Gallaher, J.L., Hilvert, D., Gelb, M.H., Stoddard, B.L., Houk, K.N., Michael, F.E., Baker, D. (2010). Computational Design of an Enzyme Catalyst for a Stereoselective Bimolecular Diels-Alder Reaction. *Science*, 329(5989):309-313.

Smith, D.B. (2000). Generating fusions to glutathione S-transferase for protein studies. *Methods Enzymol*, 326:254-270.

Song, J.K., Rhee, J.S. (2001). Enhancement of stability and activity of phospholipase A(1) in organic solvents by directed evolution. *Biochem Biophys Acta*, 11;1547(2):370-378.

Spiezia, M.C., Chiarabelli, C., Polticelli, F. (2012). Recombinant expression and insecticidal properties of a *Conus ventricosus* conotoxin-GST fusion protein. *Toxicon*, 60:744-751.

Stemmer, W.P.C. (1994). Rapid evolution of a protein in vitro by DNA shuffling. *Nature*, 370:389–391.

Stemmer, W.P.C. (1994). DNA shuffling by random fragmentation and reassembly: in vitro recombination for molecular evolution. *Proc Natl Acad Sci USA*, 91: 10747-10751.

Stemmer, W.P.C., Holland, B. (2003). Survival of the fittest molecule. *American Science*, 91:526-533.

Suen, W.C., Zhang, N., Xiao, L., Madison, V., Zaks, A. (2004). Improved activity and thermal stability of *Candida Antarctica* lipase B by DNA family shuffling. *Prot Eng Des Sel*, 17(2):133-140.

Terlau, H., Olivera, B.M., (2004). Conus venom: a rich source of novel ion channel-targeted peptides. *Physiol Rev*, 84:41–68.

Tian, Y., Mao, L., Okajima, T., Ohsaka, T. (2002). Superoxide dismutase-based third-generation biosensor for superoxide anion. *Anal Chem*, 74(10):2428-34.

Tolmachev, V., Orlova, A., Pehrson, R., Galli, J., Baastrup, B., Andersson, K., Sandström, M., Rosik, D. (2007). Radionuclide therapy of HER2-positive microxenografts using a 177Lu-labeled HER2-specific Affibody molecule. *Cancer Res*, 67(6):2773–82.

Thorstholm, L., Craik, D.J. (2012). Cyclotides as templates in drug design. *Drug Disc Today: Technologies*, 9(1):e13-e21.

Ulmer, K.M. (1983). Protein engineering. *Science*, 219(4585):666-671.

Vallin, M., Syren, P.O., Hult, K. (2010). Mutant Lipase-Catalyzed Kinetic Resolution of Bulky Phenyl Alkyl sec-Alcohols: A Thermodynamic Analysis of Enantioselectivity. C*hem Biochem*, 11(3):411-416.

Verma, N., Singh, M. (2005). Biosensors for heavy metals. *Biometals*, 18(2):121-129.

Vita, C., Roumestand, C., Toma, F., Mènez, A. (1995). Scorpion toxins as natural scaffolds for protein engineering. *Proc Natl Acad Sci*, 92:6404–6408.

Wahlberg, E., Lendel, C., Helgstrand, M., Allard, P., Dincbas-Renqvist, V., Hedqvist, A., Berglund, H., Nygren, P.A., Härd, T. (2002). An affibody in

complex with a target protein: Structure and coupled folding. *PNAS*, 100(6): 3185-3190.

Wargacki, A.J., Leonard, E., Win, M.N., Regitsky, D.D., Santos, C.N., Kim, P.B., Cooper, S.R., Raisner, R.M., Herman, A., Sivitz, A.B., Lakshmanaswamy, A., Kashiyama, Y., Baker, D., Yoshikuni, Y. (2012). An engineered microbial platform for direct biofuel production from brown macroalgae. *Science*, 335(6066):308-13.

Wermeling, D.P., 2005. Ziconotide, an intrathecally administered N-type calcium channel antagonist for the treatment of chronic pain. *Pharmacotheraphy*, 25:1084–1094.

Zhao, H., Giver, L., Shao, Z., Affholter, J.A., Arnold, F.H. (1998). Molecular evolution by staggered extension process (StEP) in vitro recombination. *Nat Biotechnol*, 16(3):258-61.

Zhang, N., Stewart, B.G., Moore, J.C., Greasham, R.L., Robinson, D.K., Buckland, B.C., Lee, C. (2000). Directed Evolution of Toluene Dioxygenase from *Pseudomonas putida* for Improved Selectivity Toward cis-Indandiol during Indene Bioconversion. *Metab Eng*, 2(4):339-348.

Toxicon 60 (2012) 744–751

Contents lists available at SciVerse ScienceDirect

Toxicon

journal homepage: www.elsevier.com/locate/toxicon

Recombinant expression and insecticidal properties of a *Conus ventricosus* conotoxin-GST fusion protein

Maria Carolina Spiezia [a], Cristiano Chiarabelli [a], Fabio Polticelli [a,b,*]

[a] Department of Biology, University of Roma Tre, Viale Guglielmo Marconi 446, 00146 Rome, Italy
[b] National Institute of Nuclear Physics, Roma Tre Section, Via della Vasca Navale 84, 00146 Rome, Italy

ARTICLE INFO

Article history:
Received 19 January 2012
Received in revised form 4 May 2012
Accepted 13 June 2012
Available online 21 June 2012

Keywords:
Conotoxins
Ion channels
Recombinant expression
Conus ventricosus

ABSTRACT

A novel conotoxin, conotoxin Vn2, was recently isolated from the venom of *Conus ventricosus*, a worm-hunting cone snail species living in the Mediterranean Sea. Analysis of conotoxin Vn2 amino acid sequence suggested that it is a member of the O1 superfamily of conotoxins. Conotoxin Vn2 displays quite a high degree of sequence similarity with bioactive peptides targeting calcium channels and in particular with the ω conotoxin PnVIB, extracted from the venom of the molluscivorous cone snail *Conus pennaceus*. In this work we describe the development of a heterologous expression system to obtain a glutathione-S-transferase (GST) fusion product of conotoxin Vn2 in a pure form and in a sufficient amount to characterize its bioactivity. The fusion product has been expressed in recombinant form in *Escherichia coli* cells, purified, and its neurotoxic activity has been assayed on the larvae of the moth *Galleria mellonella*, a simple experimental model to test the toxicity of compounds in insects. Moreover the conotoxin Vn2 Asp2His mutant has been produced to analyse the role of this aspartic acid residue in the toxin bioactivity, as an acidic amino acid is conserved in this position in all the O1 superfamily *C. ventricosus* conotoxins. Results obtained indicate that indeed conotoxin Vn2 has strong insecticidal properties at a dose of only 100 pmol/g of body weight. Surprisingly, mutation of Asp2 to His leads to enhanced toxicity in the larvae model system opening up interesting possibilities for the use of conotoxin Vn2 variants in environmental friendly crop protection applications.

1. Introduction

Cone snails are predator marine mollusks that use their venom to capture preys as well as to interact with predators and competitors. Their venom is a complex mixture of different types of (macro)molecules (Craig et al., 1999; Raybaudi Massilia et al., 2002), but in all the species the most abundant component is represented by conotoxins, small disulfide-rich neuropeptides (Olivera et al., 1991). The venom of a single cone snail species can contain up to 200 different conotoxins and, since more than 500 cone snails species are known, it has been estimated that there are about 100,000 toxins each one with specific pharmacologic properties (Terlau and Olivera, 2004). Because of their high capability to discriminate different subtypes of their molecular target, mainly ion channels classes (Olivera et al., 1990; Olivera, 2002), conotoxins have attracted much interest as tools for neuroscience research and as leads in drugs development (Olivera, 1997; Olivera et al., 1999; Adams et al., 1999). Currently the ω-conotoxin MVIIA from *Conus magus* is used as analgesic drug in its synthetic analogue Ziconotide (Miljanich, 1997; Wermeling, 2005). On the contrary, the perspectives to take advantage from

Abbreviations: GST, glutathione-S-transferase; CTX, conotoxin.

* Corresponding author. Department of Biology, University of Roma Tre, Viale Guglielmo Marconi 446, 00146 Rome, Italy. Tel.: +39 06 57336362; fax: +39 06 57336321.
E-mail addresses: mspiezia@uniroma3.it (M.C. Spiezia), c.chiarabelli@uniroma3.it (C. Chiarabelli), polticel@uniroma3.it (F. Polticelli).

0041-0101/$ – see front matter © 2012 Elsevier Ltd. All rights reserved.
http://dx.doi.org/10.1016/j.toxicon.2012.06.008

the high variety and target specificity of conotoxins to develop a new generation of pesticides (the so-called "green biotechnology") are not yet well explored. This type of approach could allow to minimise biological and environmental risks due to an indiscriminate use of chemical pesticides.

According to recent classification (Kaas et al., 2010) conotoxins can be divided in gene superfamilies (A, D, I1, I2, I3, J, L, M, O1, O2, O3, P, S, T, V, Y), based on the relative conservation of the signal peptide, in cysteine framework groups, based on the number of cysteine residues and their connectivity, and pharmacological families, based on conotoxins target specificity. Thus, there are sixteen superfamilies each one divided in several families according to the presence of two or more disulphide bridges. All conotoxins are initially expressed as a large precursor peptides that undergo post-translational modification to yield the mature toxin, typically 10–40 amino acids long, with an unusually high frequency of non-standard amino acids (Buczek et al., 2005).

A novel conotoxin, called Vn2, was recently identified in *Conus ventricosus* venom, a worm-hunting cone snail species living in the Mediterranean Sea, and its primary structure was determined (Romeo et al., 2008), revealing a cysteine framework common to I1, I3, M, O1, O2 and O3 gene superfamilies. Conotoxin Vn2 displays quite a high degree of sequence similarity with some conotoxins targeting calcium channels, in particular PnVIB from *Conus pennaceus* (Kits et al., 1996), an O1 superfamily ω-conotoxin (Fig. 1). In addition, the molecular model of conotoxin Vn2 revealed a structural similarity with the well-characterized ω-atracotoxin Hv1a, a spider toxin targeting insects high voltage activated calcium channels (Wang et al., 1999; Tedford et al., 2004).

Conotoxin Vn2 is a highly hydrophobic, 33 amino acids long peptide with a zero net charge at neutral pH (Fig. 1). The purification of conotoxin Vn2 from the *C. ventricosus* venom proved to be very difficult because of the large number of specimens needed to obtain a sufficient amount of venom to process. In fact, *C. ventricosus* cone snail is very small and its length usually does not exceed 2–3 cm (Fig. 1). Further, the unusual high hydrophobicity of conotoxin Vn2 and its net charge dramatically decrease its solubility and leads to very low sample recovery after each purification step, preventing thorough characterization of this peptide. To overcome this problem a heterologous expression system was developed in order to obtain a GST-conotoxin Vn2 fusion protein in a pure form and in a sufficient amount to characterize its bioactivity.

GST-Conotoxin Vn2 has been purified and its neurotoxic activity has been assayed on the larvae of the moth *Galleria mellonella*, a simple experimental model to test the toxicity of compounds in insects. Moreover, the conotoxin Vn2 Asp2His mutant has been produced in order to analyse the role of this aspartic acid residue in the toxin bioactivity. Results obtained indicate that indeed conotoxin Vn2 has strong insecticidal properties at a dose of only 100 pmol/g of body weight. Unexpectedly, mutation of Asp2 to His leads to enhanced toxicity in the larvae model system opening up interesting possibilities for the use of conotoxin Vn2 variants in environmental friendly crop protection applications.

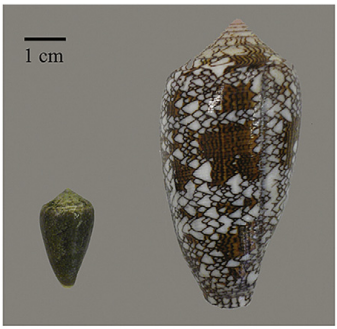


```
                                    10        20        30
Conotoxin Vn2                       EDCIAVGQLCVFWNTGRPCCSGLCVFACTVKLP
Conotoxin Vn MKLT1-01121            EDCEAGGRFCGFPKIGEPCCSGWCFFVCA----
ω-Conotoxin-like Vn MKLT1-0111      RDCVAGGHFCGFPKIGGPCCSGWCFFVCA----
Conotoxin Vn MKLT1-01122            QDCAAGGQFCGFPKIGGPCCSGWCLGVCA----
ω-Conotoxin PnVIB                   DDCEPPGNFCGMIKIGPPCCSGWCFFACA----
ω-Conotoxin-like Tx MKLT1-0223      DDCEPPGNFCGMIKIGPPCCSGWCFFACA----
ω-Conotoxin-like Tx o4              YDCEPPGNFCGMIKIGPPCCSGWCFFACA----
ω-Conotoxin-like Ar 011             --CVDGGTFCGFPKIGGPCCSGWCIFVCL----
```

Fig. 1. Top panel. Specimens of the worm-hunting *Conus ventricosus* (left) and of the mollusk-hunting *Conus textile*. Bottom panel. Multiple amino acid sequence alignment of conotoxin Vn2 and other conotoxins displaying significant sequence similarity. The sequences were retrieved by a BLAST (Schaffer et al., 2001) search over the non redundant protein sequences database, aligned using CLUSTALW-2 (Larkin et al., 2007) and visualised using Jalview (Waterhouse et al., 2009). Amino acids blocks are coloured according to BLOSUM62 score. Vn stands for *C. ventricosus*, Ar for *C. arenatus*, Pn for *C. pennaceus* and Tx for *C. textile*.

2. Materials and methods

2.1. Recombinant plasmids construction

Conotoxin Vn2 nucleotide sequence, previously cloned in pET14b plasmid (*Novagen*), was amplified with the reverse primer Rev1-ampl-conotox, and the phosphorylated forward primer F-CTX-PshAI-Asp2, using a PCR method of 35 cycles with an annealing temperature of 55 °C. The PCR product of wild type conotoxin Vn2 corresponds to the amino acid sequence EDCIAVGQLCVFWNIGRPCCSGLCVFACTVKLP. The conotoxin Vn2 Asp2His mutant was generated introducing a point mutation by PCR using the phosphorylated forward primer F-CTX-PshAI-His2 (Fig. 2).

PCR reactions were carried out using 1 μl of template 0.5 μg/μl, 4 μl of 10 mM dNTPs (*Biolabs*), 10 μl of RedTaq DNA polymerase 10× reaction buffer (*Sigma*), 4 μl of RedTaq DNA polymerase (*Sigma*), water to a final volume of 100 μl with 4 μl of the couple of primers Rev1-ampl-conotox/F-CTX-PshAI-Asp2 and Rev1-ampl-conotox/F-CTX-PshAI-His2 at a concentration of 16 pmol/μl in order to obtain, respectively, wild type conotoxin (wtCTX) and mutant conotoxin (mtCTX) nucleotide sequence. PCR products were purified from the reaction mix with Wizard SV Gel and PCR Clean-up System (*Promega*).

The final constructs were obtained cloning amplified conotoxins nucleotide sequences into the expression plasmids pET-CM (a modified pET42b plasmid (*Novagen*) created in our lab). The plasmid was digested with BamHI and PshAI Fastzyme restriction enzymes (*Fermentas*), while the whole PCR products volume was digested only with BamHI, because the forward primer displays a 5′-monophosphate end. The band corresponding to the double-digested pET-CM was excised from agarose gel and purified using Wizard SV Gel and PCR Clean-up System kit *(Promega)*. Ligations were carried out as follow: 1.5 μl T4 DNA ligase (*Fermentas*), 5 μl of ligase buffer (*Fermentas*) and 50 μl of digested plasmids and purified PCR products at 16 °C overnight to obtain pET-CM/wtCTX and pET-CM/mtCTX.

2.2. Recombinant proteins expression in E. coli

E. coli strain BL21 (DE3)pLysS ice competent cells were separately transformed with 5 μl of pET-CM/wtCTX and pET-CM/mtCTX for overproduction of GST-toxin fusion proteins. Over-night cultures were refreshed in 300 ml of YT 2× medium supplied with kanamycin and chloramphenicol (*Fluka*) antibiotics at a concentration of 25 μg/ml and 34 μg/ml respectively and left growing at 37 °C under shaking until they reached $OD_{600} = 0.8$. The expression of fusion proteins was induced adding *isopropyl β-D-1-thiogalactopyranoside* (IPTG) (*Fluka)* at a final concentration of 0.1 mM. Cells obtained from a 300 ml cultures were harvested after an over-night induction at 21 °C. The frozen pellets were mechanically lysed with alumina (*Sigma*) at 4 °C, adding a two-fold weight of alumina for each g of cells recovered after centrifugation. The soluble fraction was recovered resuspending the lysed cells in PBS 1×, EDTA 5 mM, Tween20 0.05% buffer in a volume ten-fold the total weight of cells and alumina (100 ml of buffer for each 10 g of cells and alumina. After a centrifugation at 9000 rpm at 4 °C for 30 min, the pellet was resuspended in the same volume of buffer used previously, and centrifuged again at 9000 rpm in the same conditions. The cytosolic soluble fraction of cells expressing recombinant conotoxins was treated with the protease inhibitor benzamidine, at a final concentration of 0.5 mM. In addition DL-dithiothreitol (*Sigma*) was also added at a final concentration of 10 mM, in order to maintain GST-CTXs in reduced form, and to avoid the possibility of uncorrected disulfide bridges formation and or covalent aggregation.

2.3. Recombinant proteins purification protocol

Both GST-wtCTX and GST-mtCTX recombinant proteins were purified by affinity chromatography, loading the cytosolic fraction into a GSTrap Hp column *(GE Healthcare)*. Unbounded fraction was recovered at 1 ml/min flow rate using the binding/washing buffer PBS 1× (NaCl 140 mM, KCl 2.7 mM, Na_2HPO_4 10 mM, KH_2PO_4 1.8 mM), DTT 10 mM, pH 7.3. Recombinant conotoxins were eluted at 0.7 ml/min flow

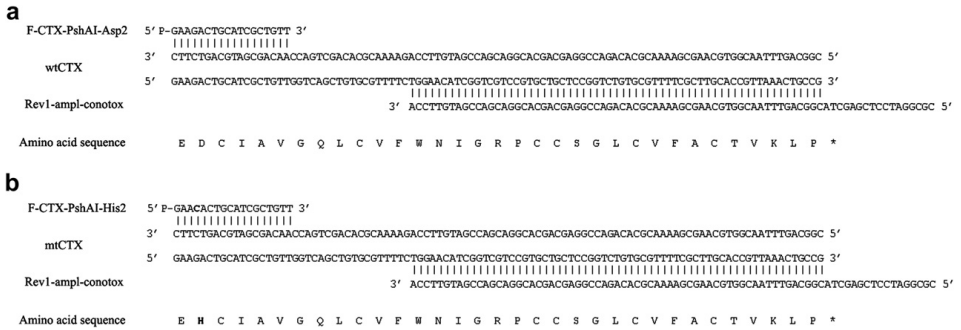

Fig. 2. The synthesized primers used to amplify the mature conotoxin Vn2 nucleotide sequences (Rev1-ampl-conotox, F-CTX-PshAI-Asp2, F-CTX-PshAI-His2; see Section 2.1 for details) and the corresponding coding sequence of a) wild type conotoxin Vn2 (wtCTX) and b) Asp2His mutant conotoxin Vn2 (mtCTX). The nucleotide which causes the change of Asp2 into His is in bold.

rate in elution buffer Tris–HCl 50 mM, reduced L-glutathione (*Sigma*) 10 mM, pH 8.0. Fractions of 1.5 ml each were collected. Each fraction from affinity chromatography was analysed by glycine 12% SDS PAGE using 30% acrylamide solution (37.5:1 acrylamide:*bis* acrylamide) for the presence of the band corresponding to the molecular weight of pET-CM/wtCTX (32.8 kDa) and pET-CM/mtCTX (33.0 kDa). The fractions containing recombinant conotoxins, wild type and mutant, were pooled separately, dialysed against NH_4HCO_3 0.1 M at 4 °C over night, using 12–14 kDa cut-off dialysis tube (*Visking*) and stored at −20 °C.

2.4. Glutathione-S-transferase assay

In order to evaluate the concentration of recombinant GST-CTXs in the collected fractions, the samples were assayed for the enzymatic activity of GST using the GST Tag Assay Kit (*Novagen*), according to manufacturer's instructions. Briefly, the reaction was carried out in presence of reduced glutathione free acid and *1-chloro-2,4-dinitrobenzene* (CDNB) as substrates, and the absorbance of the reaction was monitored at 340 nm for 5 min. The rate of change in A_{340} is proportional to the amount of GST present in the sample.

2.5. Biological toxicity assays

Different amount of the recombinant GST-CTXs (100, 30 and 6 pmol/g body weight) in a volume of 20 μl, were injected into the haemocoel of *G. mellonella* larvae, using 10 larvae for each concentration. The negative control consisted of 10 larvae inoculated with 20 μl of GST protein, at the same concentrations, expressed in pET-CM wild type plasmid and purified following the same protocol used for the recombinant wild type and mutant CTXs (see Section 2.3). The larvae were left in Petri's plates at 37 °C and were monitored at different intervals for toxicity consisting in larvae's epidermal colour change to dark brown. The observation was carried on till 72 h after injection, and the LD_{50} was calculated after 24 h after injection.

Biological toxicity has been also assessed on specimens of the fish *Gobius niger* by intraperitoneal injection of wild type CTX at concentrations of 100 and 30 pmol/g body weight. The negative control was the same used in the *G. mellonella* larvae experiment.

3. Results and discussion

3.1. Construction of the expression vectors

In order to clone conotoxin Vn2 sequence in the expression vector, as a first step, the nucleotide sequence corresponding to the mature wild type conotoxin was amplified by PCR using a forward primer of 18 bp annealing completely the conotoxin sequence, and a reverse primer of 80 bp, partially annealed. In detail we used two different forward primers: F-CTX-PshAI-Asp2, that allows the amplification of wild type conotoxin, and F-CTX-PshAI-His2 that instead introduces a single mutation in the amino acid sequence, changing the Asp2 residue into a His (Fig. 2). Wild type conotoxin (wtCTX) amplified with Rev1-ampl-conotox/F-CTX-PshAI-Asp2 primers and mutant CTX (mtCTX) amplified with Rev1-ampl-conotox/F-CTX-PshAI-His2 primers, gave on 2% agarose gel a band of 116 bp in length, as expected.

The choice to generate Asp2His mutant of conotoxin Vn2 derives from the observation that all available *C. ventricosus* conotoxins sequences display as the only conserved charged residue an acidic residue preceding the first cysteine residue of the amino acid sequence. In detail, a BLASTp (Schaffer et al., 2001) search over the non redundant database, using conotoxin Vn2 amino acid sequence as a bait, retrieves nine sequences of conotoxins, belonging to *C. ventricosus*, *Conus textile*, *C. pennaceus* and *Conus arenatus*. Multiple sequence alignment performed with ClustalW-2 (Larkin et al., 2007) highlights a cysteine framework common to I1, I3, M, O1, O2 and O3 gene superfamilies. Interestingly, the conservation of hydrophobic residues in loop 2 and 4, where the epitopes known to be involved in ω-conotoxins binding to their target are present, is also observed (Nielsen et al., 1999; Kim et al., 1994; Lew et al., 1997). In addition, seven sequences out of nine display the conservation of an acidic residue before the first cysteine (Fig. 1).

The high degree of hydrophobicity of conotoxin Vn2 required the use of a strategy to express it in soluble and active form. Therefore the choice of vector, host for the expression and growth parameters were optimized to increase the yield in soluble protein and avoid the possibility of its precipitation and/or aggregation. pET-CM plasmids represents a good choice to obtain this goal because it is designed to ensure high yield in expression of heterologous proteins as recombinant product fused to a tag protein, in this case GST. GST is not only very soluble itself, but allows easy purification and detection of recombinant conotoxins by affinity chromatography and GST activity assay. *Schistosoma japonicum* GST nucleotide sequence is located into the plasmids upstream the 5′ end of conotoxin nucleotide sequence. Between GST and conotoxin there is a linker of 35 residues. The linker on one hand ensures the folding of conotoxin avoiding steric interference with GST, on the other hand it contains two His-tag, making it possible to purify the recombinant proteins also by His-tag using a suitable affinity chromatography. In addition, downstream the linker, and so immediately upstream the conotoxin sequence, a cleavage site for Factor Xa protease (IEGR) is present for an optional cleavage of the GST tag (Fig. 3).

3.2. Expression and purification of recombinant wild type and mutant conotoxins

To improve the expression of the disulfide-rich conotoxins in their correct native state, besides to use GST as a fusion partner, which is known has positive effects on protein folding and solubility (Baneyx, 1999), we tested different conditions to optimize the yield in soluble recombinant conotoxins. The best results were obtained using an enriched growth medium (YT 2×), low concentration of inductor (IPTG 0.1 mM), low temperature (21 °C) and longer growth period (over night) for the induction. These conditions gave high expression levels of both GST-

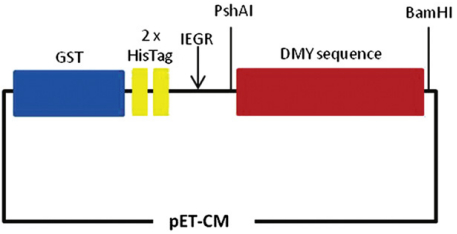

Fig. 3. Schematic representation of the plasmid used for the expression of wild type and mutant conotoxins as GST fusion proteins. Both conotoxins were cloned into pET-CM plasmid cut with PshAI and BamHI restriction enzymes. The digestion allows to eliminate the DMY sequence, to yield pET-CM/wtCTX and pET-CM/mtCTX recombinant plasmids.

conotoxins in a more soluble form, without any effects on bacterial growth. In fact, 12% SDS-PAGE analysis of induced and non induced *E. coli* cells, shows intense bands in correspondence of GST-wtCTX and GST-mtCTX molecular weight (32.8 kDa and 33.0 kDa, respectively) only in the cytosolic fraction of the induced cells transformed with the recombinant plasmids. Only very weak bands are present in the membrane fraction (Fig. 4).

The overexpressed GST-conotoxins were purified on GSTrap HP column in one step directly from the cytosolic fraction, previously adding 10 mM DTT to the samples, in order to maintain the cysteine residues in a reduced state, thus avoiding the disulfide shuffling, and significantly

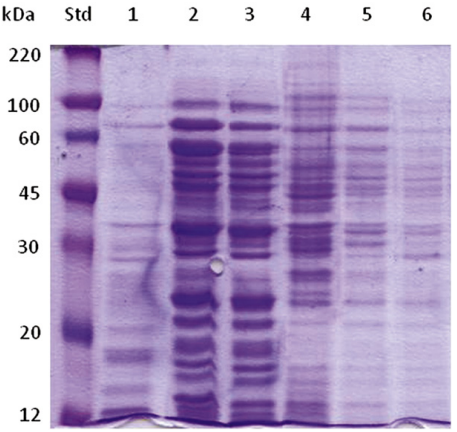

Fig. 4. SDS PAGE analysis of recombinant conotoxins GST-wtCTX and GST-mtCTX expressed in *E. coli* BL21 DE3 pLysS cells. Std: standard protein marker ColourBurst Low range (*Sigma*); lane 1: cytosolic fraction of *E. coli* cells with pET-CM plasmid not induced (negative control); lane 2: cytosolic proteins of induced *E. coli* cells transformed with pET-CM/wtCTX plasmid; lane 3: cytosolic proteins of induced *E. coli* cells transformed with pET-CM/mtCTX plasmid; lane 4: membrane fraction of negative control; lane 5: membrane fraction from induced *E. coli* cells with pET-CM/wtCTX; lane 6: membrane fraction from induced *E. coli* cells with pET-CM/mtCTX.

increasing binding of GST-conotoxins. Most of the *E. coli* proteins were recovered in the unbound fraction, collected washing the column with binding/washing buffer (PBS 1×, DTT 10 mM, pH 7.3), while recombinant conotoxins were eluted with the elution buffer Tris HCl 50 mM pH 8.0, containing 10 mM reduced glutathione. Finally the fractions from the affinity chromatography were analysed on 12% SDS PAGE. Both GST-wtCTX (Fig. 5a) and GST-mtCTX (Fig. 5b) were present in a single fraction.

The concentration of recombinant CTXs in the fractions from affinity chromatography was measured using a GST activity assay, which allows to estimate the concentration of GST fusion protein. For this reason, prior to perform the toxicity assays, the folding/oxidation process of purified GST-wtCTX and GST-mtCTX was achieved dialysing diluted solutions of the CTXs against a 0.1 M NH_4HCO_3 solution overnight at 4 °C. This procedure minimises the probability of formation of intermolecular disulphide bridges while facilitating the following concentration of the sample by lyophilization thanks to the volatility of NH_3 and CO_2.

3.3. Biological activity assays

The biological activity of recombinant CTXs was assayed injecting different amounts of GST-wtCTX and GST-mtCTX into the haemocoel of the wax moth *G. mellonella* larvae. *G. mellonella* larvae are an attractive experimental model for testing the toxicity of chemical compounds in insects due to their easy handling, low cost, and low maintenance. This system allowed us to easily measure the toxicity of GST-CTXs, because larvae's epidermal colour changes from white/grey to dark brown as result of humoral response against pathogens and toxic peptides (Jackson et al., 2009). At high concentrations of GST-wtCTX (100 and 60 pmol), immediately after injection, the larvae showed the symptoms caused by neurotoxins envenomation such as tremor and uncontrolled movements (Khan et al., 2006). On the contrary in the control experiments, larvae treated with the same concentrations of GST were unaffected even 72 h after injection. The LD_{50} at 24 h was determined to be more then 100 pmol/g body weight for GST-wtCTX and comprised between 100 and 30 pmol/g body weight for GST-mtCTX (Fig. 6). These results clearly indicate that conotoxin Vn2, expressed in the heterologous system as a GST fusion protein, retains its bioactivity.

Regarding the variability of the larvae response in the toxicity assay, several considerations can be done. First, *G. mellonella* larvae are not the natural preys of *C. ventricosus*, and therefore their molecular targets probably display structural differences with respect to the natural targets of *C. ventricosus* conotoxins (ion channels and receptors of marine polychaetes). Second, larvae at different days of larval stage could be differentially susceptible to GST-CTXs neurotoxic action. Third, the presence of proteases into the hemolymph of larvae may affect the biological activity of recombinant conotoxins, reducing their action. In addition, the recombinant expression in *E. coli* system doesn't ensure the amidation at C-terminal end of recombinant conotoxins, and it is known that the post-translational modifications play an important role for conotoxins activity (Buczek et al., 2005).

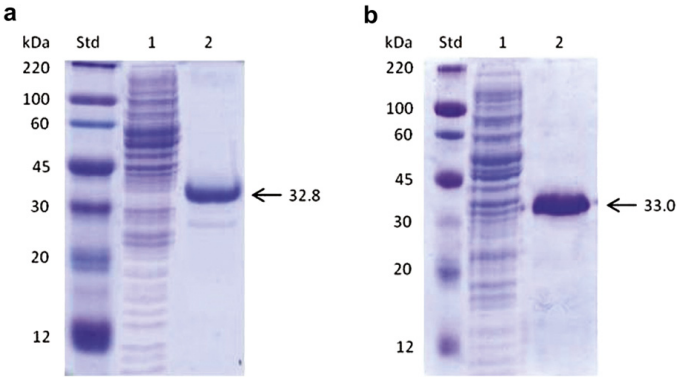

Fig. 5. SDS PAGE analysis of purified recombinant CTXs from affinity chromatography on GSTrap HP column. (a) GST-wtCTX and (b) GST-mtCTX. Std: standard protein marker ColourBurst Low range (*Sigma*); lane 1: unbound fraction; lane 2: eluted proteins.

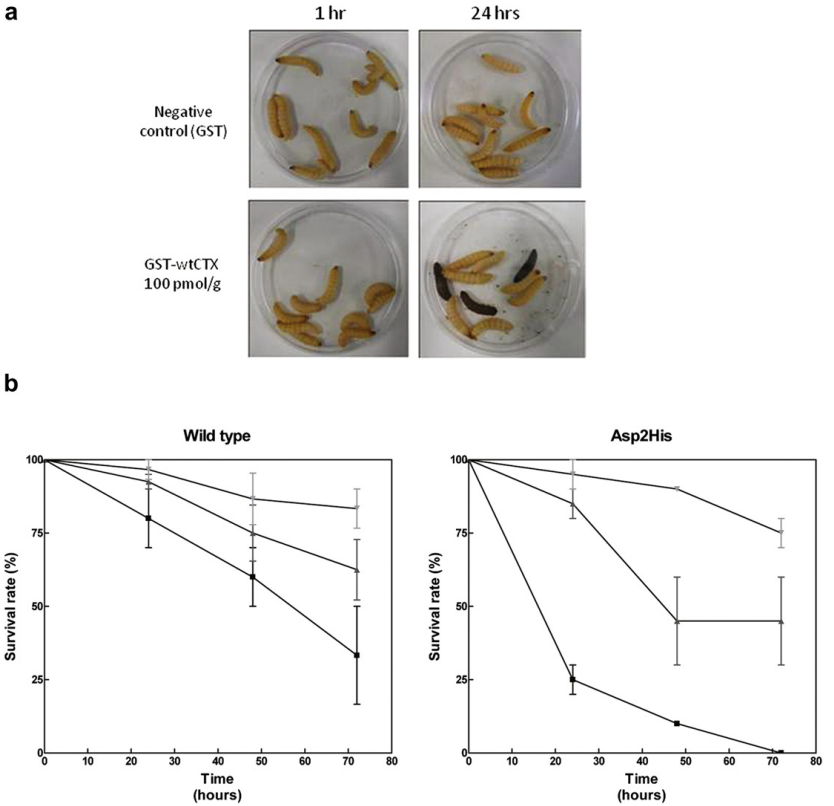

Fig. 6. Insecticidal activity of recombinant GST-CTXs on *G. mellonella* larvae. (a) an example of the colour-changing response to GST-CTXs toxicity. The lower panel shows the larvae at $T = 0$ and $T = 24$ h after injection with 100 pmol/g of GST-wtCTX; the upper panel shows the negative control (GST) monitored at the same time. (b) The survival percentage of *G. mellonella* larvae injected with 6 (light grey reversed triangles), 30 (dark grey triangles) and 100 pmol/g body weight (black squares) of purified recombinant GST-CTXs monitored at 1, 24, 48 and 72 h after treatment. The LD_{50} values at 24 h after injection calculated for GST-wtCTX and GST-mtCTX were found to be >100 pmol/g body weight and between 100 and 30 pmol/g body weight, respectively.

The wild type GST-CTX was assayed on a vertebrate model system as well, the fish *G. niger* (data not shown). Intraperitoneal injection of the conotoxin at a dose of 100 pmol/g of body weight initially and for a few seconds caused frenzy swimming behaviour of the fish, followed by full extension of ventral, dorsal and caudal fins and change in posture from horizontal to vertical. Progressive paralysis and breathing difficulties led to the death of the fish within 3 min. Injection of a lower dose (30 pmol/g body weight) caused the same initial symptoms (full extension of the fins, change in posture and breathing difficulties) but the fish fully recovered after approximately 3 h. Injection of the GST negative control at the same concentrations did not cause any detectable effect on the fish.

4. Conclusion

Conotoxins represent attractive tools to investigate the function of ion channels and receptors and to modulate their activity in central nervous system pathogenic states (Miljanich, 1997; Olivera et al., 1999; Adams et al., 1999; Shen et al., 2000; Alonso et al., 2003; Wermeling, 2005). On the contrary, the exploitation of conotoxins for biotechnological purposes is a less explored field of investigation. From this viewpoint, worm hunting cone snails possess an array of toxins that act on invertebrate ion channels and receptors and their activity in insects model systems has been demonstrated (Raybaudi Massilia et al., 2003). As one of the major challenges for modern agriculture is to achieve increased crop yields in a sustainable and cost-effective way, the perspective of using conotoxins from worm hunting cone snail species to develop insect-resistant crops is a fascinating one. This type of approach could contribute to minimise the biological and environmental risks connected with the current indiscriminate use of chemical pesticides.

In this paper we described the recombinant expression of a GST fusion construct of a novel conotoxin, called conotoxin Vn2, and we demonstrated that the fusion protein is highly toxic in an insect model system at a concentration of only few tens of pmol/g of body weight. Further, the Asp2His variant of conotoxin Vn2 is even more toxic than the wild type one, opening up the possibility to use conotoxin variants in the development of insect-resistant transgenic crops. It must be emphasized that, due to the extreme hydrophobicity of the toxin, its isolation through proteolytic cleavage of the fusion product was not possible and thus our approach does not solve the toxin supply problem. However, in view of the demonstrated bioactivity of the fusion product, this should not be a problem in the development of transgenic crops. Currently, expression in tobacco plants of the wild type and Asp2His variant of conotoxin Vn2 is in progress in order to evaluate this possibility by challenging the transgenic plants with phytophagous *Manduca sexta* (Tobacco Hornworm) larvae.

Acknowledgements

Authors wish to thank the University of Roma Tre for financial support and Prof. Paolo Mariottini for help in performing the biological activity assays in fishes.

Ethical statement

The authors declare that the study reported in the manuscript has been conducted in accordance with Elsevier ethical guidelines.

Conflict of interest statement

The authors declare no competing interests.

References

Adams, D.J., Alewood, P.F., Craik, D.J., Drinkwater, R.D., Lewis, R.J., 1999. Conotoxins and their potential pharmaceutical applications. Drug Develop. Res. 46, 219–234.

Alonso, D., Khalil, Z., Satkunanthan, N., Livett, B.G., 2003. Drugs from the Sea: conotoxins as drug leads for neurophatic pain and other neurological conditions. Mini Rev. Med. Chem. 3, 785–787.

Baneyx, F., 1999. Recombinant protein expression in *Escherichia coli*. Curr. Opin. Biotechnol. 10, 411–421.

Buczek, O., Bulaj, G., Olivera, B.M., 2005. Conotoxins and the post-translational modification of secreted gene products. Cell. Mol. Life Sci. 62, 3067–3079.

Craig, A.G., Norberg, T., Griffin, D., Hoeger, C., Akhtar, M., Schmidt, K., Low, W., Dykert, J., Richelson, E., Navarro, V., Mazella, J., Watkins, M., Hillyard, D., Imperial, J., Cruz, L.J., Olivera, B.M., 1999. Contulakin-G, an O-glycosilated invertebrated neurotensin. J. Biol. Chem. 274, 13752–13759.

Jackson, J.C., Higgins, L.A., Lin, X., 2009. Conidiation color mutants of *Aspergillus fumigatus* are highly pathogenic to the heterologous insect host *Galleria mellonella*. PLoS One 4, e4224.

Kaas, Q., Westermann, J.C., Craik, D.J., 2010. Conopeptide characterization and classifications: an analysis using ConoServer. Toxicon 55, 1491–1509.

Khan, S.A., Zafar, Y., Briddor, R.W., Malik, K.A., Mukhtar, Z., 2006. Spider venom toxin protects plants from insect attack. Transgenic Res. 15, 349–357.

Kim, J.I., Takahashi, M., Ogura, A., Kohno, T., Kudo, Y., Sato, K., 1994. Hydroxyl group of Tyr13 is essential for the activity of omega-conotoxin GVIA, a peptide toxin for N-type calcium channel. J. Biol. Chem. 269, 23876–23878.

Kits, K.S., Lodder, J.C., van der Schors, R.C., Wan Li, K., Geraerts, W.P.M., Fainzilber, M., 1996. Novel ω conotoxins block dihydropyridine-insensitive high voltage-activated calcium channels in molluscan neurons. J. Neurochem. 67, 2155–2163.

Larkin, M.A., Blackshields, G., Brown, N.P., Chenna, R., McGettigan, P.A., McWilliam, H., Valentin, F., Wallace, I.M., Wilm, A., Lopez, R., Thompson, J.D., Gibson, T.J., Higgins, D.G., 2007. Clustal W and clustal X version 2.0. Bioinformatics 23, 2947–2948.

Lew, M.J., Flinn, J.P., Pallaghy, P.K., Murphy, R., Whorlow, S.L., Wright, C.E., Norton, R.S., Angus, J.A., 1997. Structure-function relationships of ω-conotoxin GVIA. J. Biol. Chem. 272, 12014–12023.

Miljanich, G.P., 1997. Venom peptides as human pharmaceuticals. Science & Medicine 4, 6–15.

Nielsen, K.J., Adams, D., Thomas, L., Bond, T., Alewood, P.K., Craik, D.J., Lewis, R.J., 1999. Structure-activity relationship of omega-conotoxins MVIIA, MVIIC and 14 loop slice hybrids at N and P/Q-type calcium channels. J. Mol. Biol. 289, 1405–1421.

Olivera, B.M., Rivier, J., Clark, C., Ramilo, C.A., Corpuz, G.P., Abogadie, F.C., Mena, E.E., Woodward, S.R., Hillyard, D.R., Cruz, L.J., 1990. Diversity of *Conus* neuropeptides. Science 249, 257–263.

Olivera, B.M., Rivier, J., Scott, J.K., Hillyard, D.R., Cruz, L.J., 1991. Conotoxins. J. Biol. Chem. 266, 22067–22070.

Olivera, B.M., 1997. *Conus* venom peptides, receptor and ion channel target and drug design: 50 million years of neuropharmacology. Mol. Biol. Cell. 8, 2101–2109.

Olivera, B.M., Walker, C., Cartier, G.E., Hooper, D., Santos, A.D., Schoenfeld, R., Shetty, R., Watkins, M., Bandyopadhyay, P., Hillyard, D. R., 1999. Speciation of *Cone* snails and interspecific hyperdivergence of their venom peptides: potential evolutionary significance of intron. Ann. N. Y. Acad. Sci. 870, 223–237.

Olivera, B.M., 2002. *Conus* venom peptides: reflections from the biology of clades and species. Ann. Rev. Ecol. Syst. 33, 25–47.

Raybaudi Massilia, G., Eliseo, T., Grolleau, F., Lapied, B., Barbier, J., Bournaud, R., Molgó, J., Cicero, D.O., Paci, M., Schininà, M.E., Ascenzi, P.,

Polticelli, F., 2003. Contryphan-Vn: a modulator of Ca2+-dependent K+ channels. Biochem. Biophys. Res. Commun. 303, 238–246.
Raybaudi Massilia, G., Schininà, M.E., Ascenzi, P., Polticelli, F., 2002. Conopeptides: structure and function. Recent Res. Devel. Biochem. 3, 113–128.
Romeo, C., Di Francesco, L., Oliverio, M., Palazzo, P., Massilia, G.R., Ascenzi, P., Polticelli, F., Schininà, M.E., 2008. *Conus ventricosus* venom peptides profiling by HPLC-ms: a new insight in the intraspecific variation. J. Sep. Sci. 31, 488–498.
Schaffer, A.A., Aravind, L., Madden, T.L., Shavirin, S., Spouge, J.L., Wolf, Y.I., Koonin, E.V., Altschul, S.F., 2001. Improving the accuracy of PSI-BLAST protein database searches with composition-based statistics and other refinements. Nucleic Acids Res. 29, 2994–3005.
Shen, G.S., Layer, R.T., McCabe, R.T., 2000. Conopeptides: from deadly venoms to novel therapeutics. Drug Discov. Today 5, 98–106.
Tedford, H.W., Gilles, N., Ménez, A., Doering, C.J., Zamponi, G.W., King, G.F., 2004. Scanning mutagenesis of ω-Atracotoxin-Hv1a reveals a spatially restricted epitope that confers selective activity against insect calcium channels. J. Biol. Chem. 279, 44133–44140.
Terlau, H., Olivera, B.M., 2004. *Conus* venom: a rich source of novel ion channel-targeted peptides. Physiol. Rev. 84, 41–68.
Wang, X., Smith, R., Fletcher, J.I., Wilson, H., Wood, C.J., Howden, M.E., King, G.F., 1999. Structure-function studies of ω-atracotoxin, a potent antagonist of insect voltage-gated calcium channels. Eur. J. Biochem. 264, 488–494.
Waterhouse, A., Procter, J., Martin, D., Clamp, M., Barton, G., 2009. Jalview Version 2-a multiple sequence alignment editor and analysis workbench. Bioinformatics 25, 1189–1191.
Wermeling, D.P., 2005. Ziconotide, an intrathecally administered N-type calcium channel antagonist for the treatment of chronic pain. Pharmacotheraphy 25, 1084–1094.

OPEN ACCESS Freely available online

PLoS one

Cupricyclins, Novel Redox-Active Metallopeptides Based on Conotoxins Scaffold

Marco Barba[1], Anatoli P. Sobolev[2], Veranika Zobnina[1], Maria Carmela Bonaccorsi di Patti[3], Laura Cervoni[3], Maria Carolina Spiezia[1], M. Eugenia Schininà[3], Donatella Pietraforte[4], Luisa Mannina[2,5], Giovanni Musci[1,6], Fabio Polticelli[1,7]*

1 Department of Biology, University Roma Tre, Rome, Italy, **2** Institute of Chemical Methodologies, CNR, Monterotondo Stazione, Italy, **3** Department of Biochemical Sciences, Sapienza University of Rome, Rome, Italy, **4** Department of Cell Biology and Neurosciences, Istituto Superiore di Sanità, Rome, Italy, **5** Department of Drug Sciences and Technologies, Sapienza University of Rome, Rome, Italy, **6** STAAM Department, University of Molise, Campobasso, Italy, **7** National Institute of Nuclear Physics, Roma Tre Section, Rome, Italy

Abstract

Highly stable natural scaffolds which tolerate multiple amino acid substitutions represent the ideal starting point for the application of rational redesign strategies to develop new catalysts of potential biomedical and biotechnological interest. The knottins family of disulphide-constrained peptides display the desired characteristics, being highly stable and characterized by hypervariability of the inter-cysteine loops. The potential of knottins as scaffolds for the design of novel copper-based biocatalysts has been tested by engineering a metal binding site on two different variants of an ω-conotoxin, a neurotoxic peptide belonging to the knottins family. The binding site has been designed by computational modelling and the redesigned peptides have been synthesized and characterized by optical, fluorescence, electron spin resonance and nuclear magnetic resonance spectroscopy. The novel peptides, named Cupricyclin-1 and -2, bind one Cu^{2+} ion per molecule with nanomolar affinity. Cupricyclins display redox activity and catalyze the dismutation of superoxide anions with an activity comparable to that of non-peptidic superoxide dismutase mimics. We thus propose knottins as a novel scaffold for the design of catalytically-active mini metalloproteins.

Citation: Barba M, Sobolev AP, Zobnina V, Bonaccorsi di Patti MC, Cervoni L, et al. (2012) Cupricyclins, Novel Redox-Active Metallopeptides Based on Conotoxins Scaffold. PLoS ONE 7(2): e30739. doi:10.1371/journal.pone.0030739

Editor: Anna Mitraki, University of Crete, Greece

Received July 14, 2011; **Accepted** December 27, 2011; **Published** February 3, 2012

Funding: This work was supported by the italian Ministry of Education University and Research, Fund for Investments in Basic Research (http://firb.miur.it) grant no. RBAU01YMY5 to FP. The funders had no role in study design, data collection and analysis, decision to publish, or preparation of the manuscript.

Competing Interests: The authors have declared that no competing interests exist.

* E-mail: polticel@uniroma3.it

Introduction

The rational redesign of (macro)molecules based on stable scaffolds tolerant to multiple amino acid substitutions is a powerful tool to develop novel catalysts with potential biomedical and biotechnological applications [1–6]. A class of (macro)molecules which display these characteristics is the knottins family of disulphide-constrained peptides [4]. These miniproteins, tipically around 30 amino acids in length, share a peculiar knotted topology of three disulfide bridges [7]. This topology is observed in a number of evolutionary and functionally unrelated protein families including plant protease inhibitors, cone snails, snakes and spider toxins, and EGF-like domains [8]. The main structural features of knottins are their stability to thermal denaturation, resistance to proteolytic digestion, due to the cystine knot, their small size, which makes feasible their production by chemical synthesis, and a high tolerance to sequence variation of the intercysteine loops [4]. Knottins thus represent optimal scaffolds for redesign strategies aimed at developing novel metal-based catalysts.

Among knottins, the highest tolerance to sequence variability is observed in conotoxins, neurotoxic peptides from cone snails venom, frequently cited as an example of natural combinatorial chemistry [9].

In a previous study, we tested the potential of a natural 9 amino acids-long, disulphide-constrained peptide, named Contryphan-Vn [10–12], as a scaffold for the development of redox-active mini metalloproteins by computational design of two variants carrying a four-His copper binding site. The redesigned peptides, named Cupryphans, were synthesized and characterized by a variety of spectroscopic techniques, demonstrating that they selectively bind Cu^{2+} with a fairly high affinity and are endowed with superoxide dismutase activity [5].

The present study extends the work carried out on Contryphan-Vn to longer peptides, with the goal of finely modulating the stability and the catalytic activity of the redesigned metalloproteins by having a higher number of amino acid positions available to substitution. In particular, we exploited the high tolerance of conotoxins to multiple amino acid substitutions of to engineer a copper binding site in two variants of an ω-conotoxin. The design procedure took into account the position-specific conservation of the intercysteine loop residues in this family of peptides in order to facilitate spontaneous achievement of the right fold. The rationale behind this choice was that of keeping the composition of the intercysteines loop as close as possible to that of the natural sequences to favour loops conformations close to those observed in ω-conotoxins. Furthermore, the peculiarity of this work with respect to other redesign strategies employing the knottins scaffold

is that the four His metal ligands were introduced in the place of four of the six Cys residues of the natural scaffold, with the aim of avoiding multiple conformational isomers arising from incorrect cysteine pairing during oxidative folding of the peptides.

Results and Discussion

Rational design of a copper binding miniprotein based on conotoxins scaffold

The strategy employed in the present work to select a suitable scaffold for engineering a mini metalloprotein was that of deriving a consensus sequence from one of the most studied knottins families, the O superfamily of conotoxins [13]. The rationale was that of identyfing a scaffold with sequence/structural properties common to all the members of the family and thus able to spontaneously attain a stable fold. The amino acid sequence of one of the members of this family, the ω-conotoxin GVIA, which is one of the best characterized in terms of both a function and structure [14], was used as a bait in a *PSI-BLAST* [15] search of the non redundant protein sequences database to recover all protein sequences displaying a significant sequence similarity. The recovered amino acid sequences were then aligned using the *ClustalW* program [16], to obtain the multiple sequence alignment shown in figure 1A. The three-dimensional structure is also available for 6 out of the 18 conotoxins in the alignment, namely ω-conotoxin GVIA, ω-conotoxin GVIA (O10K), ω-conotoxin MVIIC, ω-conotoxin MVIIA, ω-conotoxin So3 and the ω-conotoxin TxVII (PDB codes: 2CCO, 1TR6, 1OMN, 1OMG, 1FYG, 1F3K), thus facilitating the analysis of sequence/structure relationships.

The multiple alignment was then analysed using the Weblogo program [17] to obtain the graphic representation shown in figure 1B, from which a consensus sequence of the ω-conotoxins was derived by choosing in each position of the sequence the most frequent amino acid. The consensus sequence shown in figure 1B was the starting point for the design. However, this sequence was subsequently modified taking into account the following constraints: 1) the need to limit the hydrophobicity of the designed peptide in order to avoid aggregation phenomena (this is why Ala6, Met12, Gly25 and Gly28 where changed into Ser, Ser, Lys and Tyr residues, the second most represented residues in those positions according to the weblogo plot); 2) the need to introduce a Trp probe in the designed peptide in order to measure the copper binding affinity of the peptide using fluorescence quenching techniques (this is why Tyr13 of the consensus sequence was substituted by a Trp residue); 3) the need to constrain the intercysteines loops and the C-terminal region of the peptide so as to favour correct positioning of the His residues to generate the

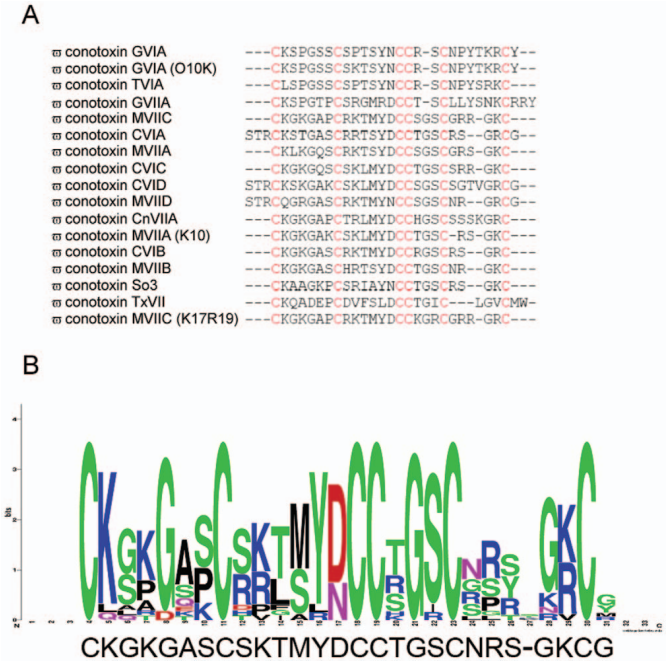

Figure 1. Amino acid sequence alignment of ω-conotoxins (A) and Weblogo [17] plot (B). The consensus sequence of the aligned ω-conotoxins is reported below the plot in panel B. The consensus sequence has been obtained by calculating the frequency of each amino acid in each position of the amino acid sequence of the aligned ω-conotoxin sequences using the Weblogo tool [17].
doi:10.1371/journal.pone.0030739.g001

copper binding site (this is why Lys10 and Arg22 were both changed to Pro residues). With these changes to the consensus sequence, the designed peptide accidentaly resulted to have a high sequence similarity to our starting bait ω-conotoxin GVIA (Figure 2). Thus, ω-conotoxin GVIA three-dimensional structure was used to construct *in silico* the structural model of the first mini metalloprotein variant (see Materials and Methods section for details). One of the main problems connected with the folding of conotoxins is the high probability of formation of multiple disulphide bonds isomers of the mature peptides. It is well known in fact that *in vivo*, folding of conotoxins occurs at the prepropeptide stage (when the mature toxin sequence has two additional sequence stretches at the N-terminus) and is aided by protein disulphide isomerases [18]. In our case, to ensure that the redesigned peptide folded in a unique structure, we substituted four of the six cysteine residues of ω-conotoxin GVIA with His residues, after verifying that the interatomic distances of the introduced His residues matched those observed in the Cu,Zn superoxide dismutase copper site [19], taken as a template.

In particular, His residues were introduced in the place of Cys8, Cys15, Cys19 and Cys26. These substitutions determine the formation of a single disulphide bridge in the peptide structure, avoiding problems due to the incorrect pairing of cysteine residues, and hence favouring a unique folding of the redesigned peptide. At the same time, binding of the metal to the four His ligands was expected to constrain the polypeptide chain in a manner similar to the two missing knotted disulphides. Furthermore, binding of copper in a solvent shielded part of the molecule was expected to facilitate the achievement of a higher superoxide dismutation rate as demonstrated in Cu,Zn superoxide dismutase [20]. In fact, the electrostatic steering effect of copper on the superoxide anion substrate is enhanced if the copper charge is not screened by the solvent [20].

The redesigned miniprotein, whose amino acid sequence is shown in figure 2, has been named Cupricyclin-1 to emphasize the presence of a copper binding site and the cyclization of the polypeptide chain through one disulphide bond.

Molecular dynamics simulations of Cupricyclin-1

The structural model of Cupricyclin-1 was subjected to a 10 ns molecular dynamics (MD) simulation run in explicit solvent to test the stability of the introduced copper site and of the overall structure (Figure 3). In detail, the solvated molecule was first energy-minimized applying position restraints to all non-hydrogen atoms. In this phase, the distances between the copper ion and the Nε2 atoms of the four coordinating His residues were restrained to a value of 2 Å by using a harmonic potential (see Materials and Methods section for details). Subsequently, 100 ps molecular dynamics simulation under NVT conditions, followed by 100 ps NPT simulation, with position restraints on all heavy atoms of the miniprotein and with restrained copper-ligand binding distances, were performed in order to equilibrate the temperature and pressure of the system. In the following step the structure was subjected to a 5 ns MD simulation with harmonic potentials applied only to the distances between copper and its ligands, and finally to a 10 ns MD simulation without any restraint. MD simulations without restraints indicated that the redesigned peptide can stably bind copper while preserving a well defined structure. Detailed analysis of the position of the copper ion with respect to the protein atoms of Cupricyclin-1 revealed that the distances between copper and the nitrogen atoms of the four ligands ranged from 2.0 to 2.5 Å over the entire course of the production run. Moreover, two additional ligands entered the copper coordination sphere during the simulation: one water molecule (metal-ligand distance 1.8–2.2 Å) and the carbonyl oxygen of Trp13 (metal-ligand distance 2.0–2.5 Å). The coordination geometry of the copper ion remained octahedral during the simulation time with an average angle between copper and each pair of adjacent ligands of approx. 90° (values ranging from 88° to 93°). The Nε2 atoms of His8, His15, His26 and the carbonyl oxygen of Trp13 lie in one plane, while the Nε2 atom of His19 and the water molecule are above and below the plane. This coordination geometry is similar to that observed in Cu,Zn superoxide dismutase (See Figure S1); indeed, a copper-coordinating water molecule is also present in this enzyme [19].

Cupricyclin-1 synthesis and characterization

Cupricyclin-1 was synthesised by standard Fmoc chemistry, loaded on a Vydac C_{18} semipreparative column and isolated from by-products by HPLC. The major peptide-containing fraction was then air oxidized at 0.01% concentration (w/w) in 0.1 M NH_4HCO_3 to allow formation of the single disulphide bond. The cyclic miniprotein was finally purified from dimers/multimers by HPLC connected with an ESI-IT mass spectrometer and

Figure 2. Amino acid sequence of ω-conotoxin GVIA (A) and of the redesigned peptides Cupricyclin-1 (B) and Cupricyclin-2 (C), see below.
doi:10.1371/journal.pone.0030739.g002

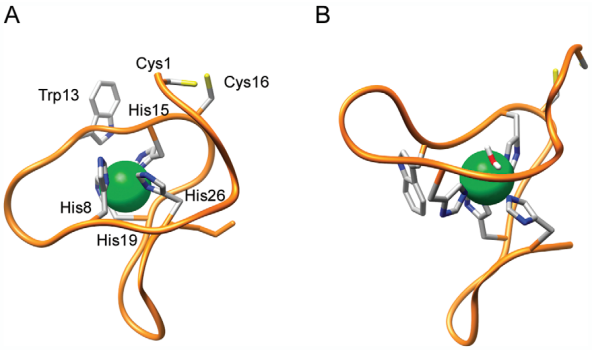

Figure 3. Three-dimensional model of Cupricyclin-1 before (A) and after MD simulations (B). The copper ion is represented by a green sphere. For clarity only the His ligands, Trp13, the two Cys residues and the copper-coordinating water molecule are shown. The figure was prepared using UCSF Chimera [53].
doi:10.1371/journal.pone.0030739.g003

eluates were collected and characterized by MALDI-TOF analysis.

The MALDI-TOF spectrum of Cupricyclin-1 shows a main peak with a mass of 3154,00 a.m.u., corresponding to Cupricyclin-1 in the cyclic oxidized form (See Figure S2A). To confirm this result Cupricyclin-1 was treated either with the alkylating agent iodoacetamide (IAM), or with dithiothreitol (DTT), or else with both DTT and IAM. In the case of IAM treatment no modification was observed in the MALDI-TOF spectrum profile (Figure S2B), while the sample treated with DTT showed, as expected, an increase of 2 a.m.u. of the main MALDI-TOF spectrum peak, consistent with reduction of the two Cys residues (Figure S2C). Finally, treatment with DTT followed by IAM yielded a main peak centered at 3270 a.m.u., corresponding to the alkylation of two Cys residues (mass increase +116 a.m.u.) (Figure S2D).

Cupricyclin-1 metal binding ability

Evidence of Cu^{2+} binding to Cupricyclin-1 was first obtained by fluorescence quenching experiments, exploiting the ability of copper ions to quench the fluorescence emitted by the single Trp residue (Trp13) upon binding to the miniprotein [5,21]. Fluorescence quenching was dependent on metal concentration and reached a maximum at a $[Cu^{2+}]/[peptide]$ of approx. 1:1 (Figure 4). These characteristics are consistent with an energy-transfer mechanism from the tryptophan residue to the copper bound at the binding site. Fluorescence quenching due to copper binding to Cupricyclin-1 was used to determine the binding affinity of the miniprotein for Cu^{2+}. The fluorescence intensity decrease at 352 nm as a function of increasing amounts of copper ions was fitted with a non linear regression curve (Figure 4), obtaining a copper dissociation constant of 3.8 ($\pm$1.4)$\times 10^{-8}$ M.

Further evidence of copper-peptide binding was obtained by optical spectroscopy analysis. Addition of a stoichiometric amount of $CuCl_2$ to Cupricyclin-1 (0.6 mM final concentration) induced the appearance of absorption bands with maxima at 300–312 nm and 520–600 nm (Figure 5), the first indicative of a Cu^{2+}-histidine charge-transfer [22], the second due to electronic transitions of copper *d-d* orbitals and typical of copper complexes with nitrogen ligands [22,23]. The calculated molar extinction coefficient of holo-Cupricyclin-1 at 595 nm is 203 M^{-1} cm^{-1}.

The stability of the copper site of Cupricyclin-1 was also investigated by differential scanning calorimetry (DSC). The DSC trace of Cupricyclin-1 with bound copper exhibited a strong exotherm beginning above 55°C and showing a minimum at 95°C. The exotherm disappeared after copper removal (see Figure S3). No clear endotherm was evident in the thermograms, due to the fact that the peptide almost completely lacks defined structural elements which can yield DSC signals (such as hydrogen bonds). In copper proteins such as azurin and plastocyanin, the exotherm is attributed to copper-dependent redox reactions with cysteines following copper release [24–26]. By analogy, DSC results indicate that the metal site of Cupricyclin-1 is stable up to 55°C and that copper release is complete only at 95°C (the $T_{1/2}$ for copper release being approx. 75°C). The stability of the copper site in Cupricyclin-1 well compares with that of natural metalloproteins such as azurin and plastocyanin which display complete copper release at temperature values ranging from 70 to 85°C depending on the metal oxidation state and the DSC scanning rate [24–26].

The fluorescent binding titration data suggested a copper:peptide stoichiometry of 1:1. However this result would also be compatible with the presence of higher cross-linked oligomers where the copper:peptide ratio is 1:1 as well. To rule out this possibility a MALDI-TOF spectrum of Cupricyclin-1 was recorded, showing that only the apo and holo monomeric forms of the peptide were present in the sample (see Figure S4).

EPR spectroscopy characterization of Cupricyclin-1

The liquid nitrogen EPR spectrum of Cupricyclin-1 (Fig. 6A, spectrum "Cc-1") appeared to arise from two spectroscopically distinguishable species of copper, as can be clearly seen by the split peak of the low magnetic field hyperfine line (arrows). The EPR parameters for a copper complex are determined by the chemical composition and the physical constraints on the atoms nearest to the metal ion, with g and A values strictly depending on the composition of the ligand atoms bound to the copper. The EPR spectrum of Cupricyclin-1, although heterogeneous, reveals an essentially axial g tensor, with $g_{//}$ values in the range 2.21–2.25.

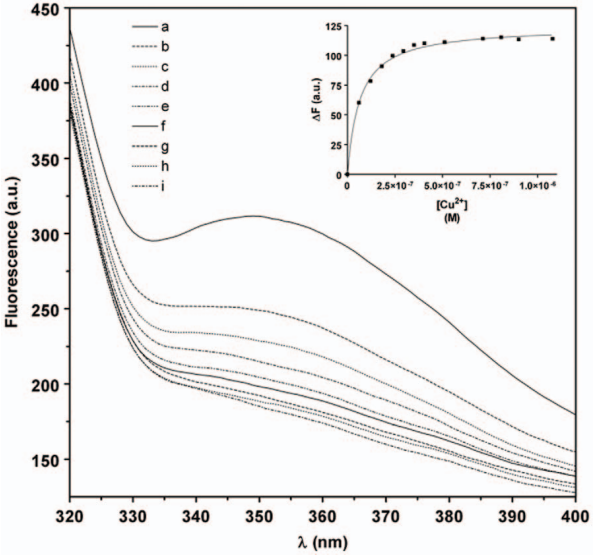

Figure 4. Emission fluorescence spectra of Cupricyclin-1 in the presence of increasing amounts of Cu^{2+} ions. (a) apo Cupricyclin-1 (0.5 μM); (b) a+$CuCl_2$ 0.06 μM; (c) a+$CuCl_2$ 0.12 μM; (d) a+$CuCl_2$ 0.18 μM; (e) a+$CuCl_2$ 0.24 μM; (f) a+$CuCl_2$ 0.30 μM; (g) a+$CuCl_2$ 0.36 μM; (h) a+$CuCl_2$ 0.41 μM and (i) a+$CuCl_2$ 0.51 μM (only the spectra relative to a stoichiometric ratio Cu^{2+}:Cupricyclin-1 ≤1 are reported); **(inset)**: Determination of the dissociation constant of Cu^{2+} to Cupricyclin-1 by fluorescence quenching experiments. The non linear fitting curve of fluorescence decrease at 352 nm as function of increasing amounts of Cu^{2+} ions is shown as a continuous line.
doi:10.1371/journal.pone.0030739.g004

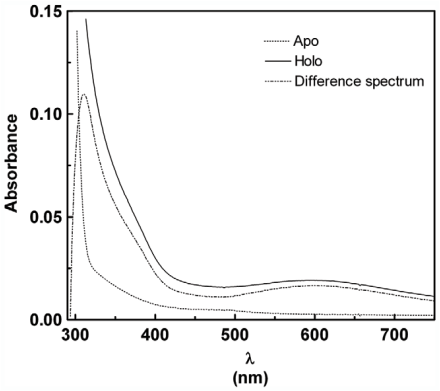

Figure 5. Optical spectra of apo and holo Cupricyclin-1 (0.6 mM in 50 mM sodium acetate buffer, pH 6.5). The difference spectrum is also shown to evidence the appearance of a band at 300–312 nm, indicative of a Cu^{2+}-histidine charge-transfer [21,22].
doi:10.1371/journal.pone.0030739.g005

The copper hyperfine values $A_{//}$, on the other hand, can be estimated to be above 0.018 cm^{-1}. These values are typical of a type-2 mono Cu(II) complex, *i.e.* a square planar ligation of the copper ion with possible additional axial ligations [27]. The empirical quotient $f = g_{//}/|A_{//}|$ is considered an index of tetrahedral distortion, ranging from 105 to 135 for square-planar copper structures [28]. In this respect, the EPR parameters of Cupricyclin-1 suggest a low degree of tetrahedral distortion. Also worth of note is the absence of an anomalous number of lines in the parallel region and of any half-field signal arising from a triplet spin state, strongly supporting the hypothesis that the peptide is monomeric in solution. All these data are fully consistent with the coordination environment predicted by MD simulations. Variable power experiments in the 2.5–190 mW range (not shown) did not discriminate between the two signals, which had similar saturation behavior, suggesting that the spectroscopic inhomogeneity could arise from slightly different conformational states in a single copper coordination environment.

Peisach and Blumberg showed that the g and A values in the parallel region of the EPR spectrum of copper sites give information on the type of ligating atoms [27]. According to their method, the parameters of Cupricyclin-1 are in agreement with a 4-nitrogen coordination sphere. This is also consistent with the nitrogen-induced superhyperfine splitting pattern observed in the closely related Cupricyclin-2 (see below).

The metal-binding region of native SOD constitutes the catalytic active site, therefore it is interesting to study in detail

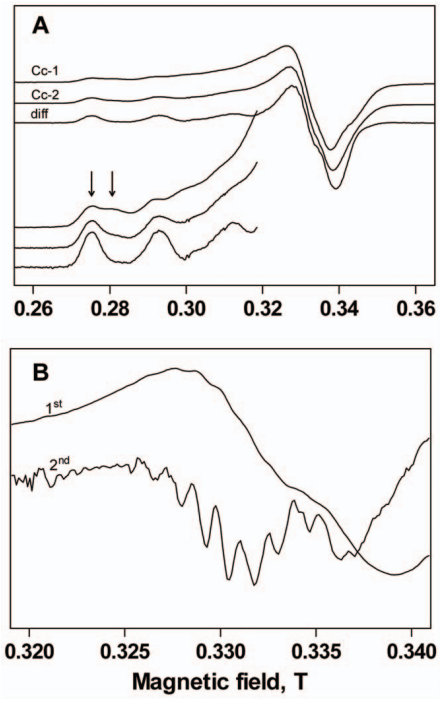

Figure 6. EPR spectrum of Cupricyclins. Panel A shows the spectra of Cupricyclin-1 (Cc-1), Cupricyclin-2 (Cc-2) and a difference spectrum (diff) obtained by arbitrarily subtracting a fraction of Cc-1 from Cc-2. Arrows on the first hyperfine of Cc-1 reveals the signal heterogeneity. Experimental details in the text. Panel B displays a detail of the perpendicular region of the difference spectrum, shown both as the standard first derivative lineshape and as the second derivative curve, to better evidence the superhyperfine lines due to interaction of copper with the four nitrogen nuclei of the coordinating histidine residues.
doi:10.1371/journal.pone.0030739.g006

the metal sites of SOD-mimics in order to correlate the structure to the biological behaviour. In the native enzyme, copper is coordinated by three imidazole residues and a water molecule, while an imidazolate bridge links the copper and zinc sites. This results in a distorted tetrahedral structure of the copper site that can be readily inferred from its strong anisotropic EPR signal [29] with an *f* value of 159 for bovine Cu,Zn SOD [30]. The site is very flexible, switching from an irregular pyramid containing one weak axial water molecule in the oxidized form to a tricoordinated conformation in its reduced form. This is a crucial aspect in that high SOD activity is related to high flexibility in the conformation around copper [31,32]. In this respect, the copper environment in Cupricyclin-1 seems to be significantly more rigid, accounting for its SOD activity that, although significant for a SOD-mimic (see below), is still far from that of the native enzyme. It should also be reminded that a five-coordinated square pyramidal or trigonal bipyramidal structure is more favourable for a good SOD activity than a four-coordinated square planar structure [33].

NMR spectroscopy characterization of Cupricyclin-1

Copper interaction with Cupricyclin-1 was also investigated by NMR spectroscopy. The assignment of the ^{1}H spectrum of apo-Cupricyclin-1 is shown in Table 1. Copper interaction with apo-Cupricyclin-1 was studied by addition of aliquots of $CuSO_4$ to a 1.06×10^{-3} M solution of the peptide in H_2O/D_2O (9:1 v/v). The first $CuSO_4$ addition (Cu^{2+}/peptide ratio 0.05:1) caused a drastic broadening of Hδ (between 7.0 and 6.9 ppm) and Hε proton signals (between 7.7 and 7.6 ppm) of the imidazole rings of all four histidine residues (see Figure 7). On the other hand, the signals of Trp, Tyr and of other amino acid residues remained unchanged. Stepwise addition of $CuSO_4$ led to a further broadening of His signals and to a decrease of the intensity and only minor broadening of other ^{1}H amino acid signals (Figure 7). At a Cu^{2+}/peptide ratio higher than 1.0 a further broadening of all ^{1}H amino acid signals was observed.

These results suggest that at low Cu^{2+}/peptide ratios ($\leq$1), a peptide–Cu^{2+} complex is formed with a specific interaction between the metal and all the four His residues of the peptide, as indicated by the broadening of histidine signals. At high Cu^{2+}/peptide ratios (>1), when the specific binding is already saturated, a nonspecific interaction between Cu^{2+} and other amino acid residues is manifested by a further, minor, intensity decrease and broadening of all the amino acid signals, as already observed in a previous study from our lab on a structurally unrelated copper-binding peptide [5].

Determination of superoxide dismutase activity of Cupricyclin-1

The ability of the copper ion bound to Cupricyclin-1 to be reversibly reduced, a prerequisite for any redox-mediated catalytic activity, was tested by assaying the superoxide dismutase activity of Cupricyclin-1 using the pyrogallol enzymatic assay [34]. From the concentration of superoxide dismutase and Cupricyclin-1 required to reach 50% inhibition of the reaction rate of pyrogallol autoxidation (2.7×10^{-9} M and 4.7×10^{-5} M, respectively, Table 2) and taking as a reference the enzymatic activity of superoxide dismutase (3.9×10^{9} M^{-1} s^{-1}) [35], a superoxide dismutation rate of 1.8×10^{5} M^{-1} s^{-1} was calculated for Cupricyclin-1, a value of the same order of magnitude of that observed for Cupryphans [5] and for non peptidic superoxide dismutase mimics [36].

Design and characterization of Cupricyclin-2

To study the role of peptide backbone flexibility in the metal binding affinity and redox properties of Cupricyclins, an additional variant was designed in which the intercysteines loop residue Pro10 was substituted with an Ala residue and a Gly residue was introduced between Arg17 and Ser18 to increase the length of the loop connecting His15 to His19 (Figure 2C). The structural properties of the novel peptide, named Cupricyclin-2, were studied through a combination of MD simulations, fluorescence, optical and EPR spectroscopy, and its superoxide dismutase activity was determined. Molecular dynamics simulations, carried out following the same protocol used for Cupricyclin-1, indicated that Cupricyclin-2 can stably bind copper in a similar geometry as that observed for Cupricyclin-1. Also in the case of Cupricyclin-2 the coordination geometry of the copper ion remains octahedral during the time of the simulations, with the nitrogen atoms of His8, His15 and His20 together with the

Table 1. Assignments of ^{1}H and ^{13}C resonances of apo-Cupriknottin 1 in D_2O at 300 K, pH 7.0.

Amino acid	Atom	Chemical shift (ppm)				
		Cα	Cβ,β′	Cγ,γ′	Cδ	Others
Asn 20	^{1}H	4.88	2.83; 2.62			
	^{13}C	49.6	37.8			
Asn 14	^{1}H	4.50	2.60			
	^{13}C	52.7	37.2			
Arg a	^{1}H	4.33	1.83; 1.74	1.58	3.12	
	^{13}C	55.2	29.4	25.8	42.0	
Arg b	^{1}H	4.26	1.65	1.49; 1.43	3.07	
	^{13}C	54.6	29.8	25.7	42.0	
Gly 3, 5	^{1}H	3.95				
	^{13}C	44.1				
His a	^{1}H	4.62	3.10; 3.01		6.93	
	^{13}C	55.3	30.0		118.8	
His b	^{1}H	4.52	3.08		6.91	
	^{13}C	55.8	29.6		118.8	
His c	^{1}H	4.58	3.04; 2.97		6.89	
	^{13}C	55.1	30.0		118.8	
His d	^{1}H	4.58	3.04; 2.98		6.87	
	^{13}C	55.1	30.0		118.8	
Lys 2, 4, 24	^{1}H	4.25; 4.24; 4.19	1.64	1.36		2.94
	^{13}C	55.0; 55.5; 55.6	27.8	23.4		40.8
Pro 10	^{1}H	4.35	2.26; 1.91	1.96	3.70	
	^{13}C	62.6	30.8	26.1	49.4	
Pro 21	^{1}H	4.32	2.13; 1.65	1.85; 1.63	3.59	
	^{13}C	62.2	30.6	25.5	49.3	
Ser 6, 7, 9, 12, 18	^{1}H	4.35; 4.41; 4.48	3.82			
	^{13}C	57.8;57.3; 57.1	62.4			
Thr a	^{1}H	4.28	4.19	1.13		
	^{13}C	60.8	68.2	20.3		
Thr b	^{1}H	4.25	4.15	1.17		
	^{13}C	60.6	68.5	20.3		
Trp 13	^{1}H	4.66	3.26; 3.21		7.19	7.56 (Hε); 7.21 (Hζ3); 7.12 (Hη); 7.46 (Hζ2)
	^{13}C	56.2	28.1		125.8	119.7 (Cε); 123.4 (Cζ3); 120.7 (Cη); 113.4 (Cζ2)
Tyr 22	^{1}H	4.58	3.11; 2.96		7.12	6.81 (Hε)
	^{13}C	56.7	36.9		131.8	117.1 (Cε)
Tyr 27	^{1}H	4.35	3.03; 2.87		7.02	6.78 (Hε)
	^{13}C	56.7	38.1		132.0	116.9 (Cε)
Cys a	^{1}H	4.61	3.18; 2.98			
	^{13}C	54.5	39.3			
Cys b	^{1}H		3.13			
	^{13}C		41.0			

Letters a, b, c, d in the first column indicate the amino acid residues whose specific position in the peptide chains was not assigned.
doi:10.1371/journal.pone.0030739.t001

carbonyl oxygen of Gly18 lying in one plane and the nitrogen atom of His27 and a water oxygen acting as apical ligands.

Comparative analysis of the MD simulations trajectories of Cupricyclin-1 and Cupricyclin-2 indicated that, indeed, substitution Pro10Ala and insertion of Gly18 changed the conformational stability and flexibility of the molecule as well as the pattern of hydrogen bond interactions and of copper-protein interactions. A decrease of the magnitude of conformational changes at the beginning of the simulation, a higher flexibility over the course of the production run as well as a decrease of the number of hydrogen bonds of Cupricyclin-2 compared to Cupricyclin-1 were observed.

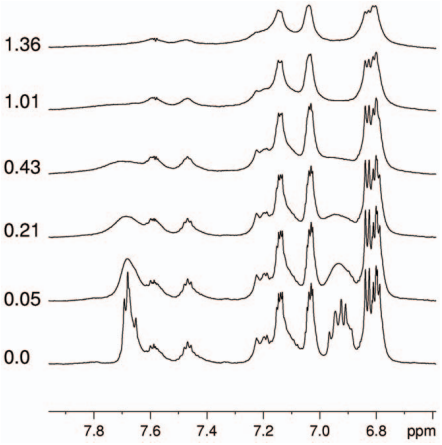

Figure 7. Titration of Cupricyclin-1 with $CuSO_4$ monitored by ^1H NMR. The molar ratio $CuSO_4$/Cupricyclin-1 is reported on the left side of each spectrum.
doi:10.1371/journal.pone.0030739.g007

Despite the similarity of the starting conformations, the distribution of RMSD values as a function of time shows that, initially, Cupricyclin-1 underwent bigger conformational changes than Cupricyclin-2 with respect to the starting conformation (see Figure S5, top panel). However, analysis of the RMSD plots indicates that, after the initial conformational changes occurred during the equilibration period, Cupricyclin-1 remained more stable than Cupricyclin-2 over the course of the production run (lower fluctuations of the RMSD values; Figure S5, top panel). It is noticeable in the RMSD plot that Cupricyclin-2 underwent a reversible structural change during the period from 4.7 to 5.7 ns of the unrestrained simulation.

Analysis of the matrix of Cα RMSD values of every frame with respect to every other frame of the production run simulation (a measure of the extent of conformational variability observed in the system) shows that Cupricyclin-1 was represented by two distinct clusters of conformations (see Figure S5, bottom panel A). A clear structural rearrangement at around 4 ns of the unrestrained run visible on the matrix representation coincides with a very small increase of the values on the RMSD plot (Figure S5, top panel). Analysis of the RMSD matrix of Cupricyclin-2 suggests that the protein underwent several reversible transitions during the simulation. Moreover, a higher similarity (lower RMSD values) between the members of the same clusters of Cupricyclin-1 than within the clusters of Cupricyclin-2 is observed (Figure S5, bottom panel B).

From fluorescence quenching experiments a copper dissociation constant of $10.7\ (\pm 1.1)\times10^{-8}$ M was determined for Cupricyclin-2, suggesting that a higher backbone flexibility causes a slight decrease of the peptide affinity for copper ions. Optical spectroscopy studies demonstrated that, also in the case of Cupricyclin-2, addition of a stoichiometric amount of $CuCl_2$ induces the appearance of absorption bands with maxima at 300–312 nm and 520–600 nm which, by analogy with Cupricyclin-1, were attributed to a Cu^{2+}-histidine charge-transfer band and to electronic transitions of copper *d-d* orbitals typical of copper complexes with nitrogen ligands, respectively [22,23]. The calculated molar extinction coefficient at 525 nm was 476 M^{-1} cm^{-1}.

Quite interestingly, the EPR spectrum of Cupricyclin-2 was much less heterogeneous than that of Cupricyclin-1 (Fig. 6A, "Cc-2" vs "Cc-1"). However, both spectra appeared to be constituted by the same species, although with different fractional contributions. As a matter of fact, a "pure" EPR lineshape was readily obtained by subtracting a fraction of the Cupricyclin-1 lineshape from the spectrum of Cupricyclin-2 (Fig. 6A, "diff"). The difference spectrum clearly showed at least nine superhyperfine lines in the perpendicular region of the spectrum (Fig. 6B), with position and average coupling constant (≈14 G) typical of copper(II) complexes with a minimum of four magnetically equivalent histidine residues on the coordination plane, this result being fully consistent with the body of our data. Again, the EPR parameters were within a four nitrogens coordination sphere, according to the Peisach-Blumberg plot [27].

Finally, the superoxide dismutase activity of Cupricyclin-2 was found to be slightly higher than that of Cupricyclin-1, the reaction rate being 3.4×10^5 M^{-1} s^{-1} as compared to 1.8×10^5 M^{-1} s^{-1} determined for Cupricyclin-1 (Table 2). This result suggests that, while a higher flexibility of the peptide backbone decreases the stability of the copper site, the same flexibility may facilitate coordination of both Cu^{2+} and Cu^{1+} within the same binding site with positive effects on the copper reduction rate and thus on the ability of the mini metalloprotein to act as a catalyst in redox reactions.

Conclusions

The use of metal-binding peptides in green chemistry applications and bioremediation is becoming an increasingly adopted strategy [37]. This is due to the fact that small stable scaffolds can be engineered to host a metal binding site starting from basic structural principles [1]. On the other hand, the insertion of metal binding residues can lead to a destabilization of the scaffold and to undesired structural changes [1]. Knottins represent one of the most stable scaffolds, being constrained by three disulphide bonds, and are extremely tolerant to sequence variation thus representing optimal candidates for redesign strategies [4]. However the presence of three disulphide bonds implies that the attainment of a unique structure during folding is severely hampered by the possible formation of multiple disulphide bonds isomers with a consequent low yield of the desired structural form [18]. To overcome this problem, in this work we have

Table 2. Superoxide dismutase activity of Cupriknottins.

	[SOD]	[Cupryphan]	[Cupriknottin-1]	[Cupriknottin-2]
50% inhibition	2.7×10^{-9} M	8.5×10^{-5} M	4.7×10^{-5} M	3.1×10^{-5} M
K_1, K_2	3.9×10^9 M^{-1} s^{-1}	1.0×10^5 M^{-1} s^{-1}	1.8×10^5 M^{-1} s^{-1}	3.4×10^5 M^{-1} s^{-1}

doi:10.1371/journal.pone.0030739.t002

adopted the strategy of substituting the two knotted disulphides of a member of the knottins family, ω-conotoxin GVIA, with a metal binding center. In this way it has been possible to obtain a rigid metal-coordination environment while at the same time avoiding the problems intrinsically connected with the presence of multiple disulphide bonds. The redesigned peptides Cupricyclin-1 and -2 bind copper ions with a fairly high affinity and display reversible reduction of the copper center, catalyzing the dismutation of superoxide anions at an acceptable rate, compared to other superoxide dismutase mimics [5,36]. One way of improving the catalytic efficiency of Cupricyclins would be that of mimicking the electrostatic potential distribution observed in Cu,Zn superoxide dismutases in which a positively charged active site is hosted in an essentially negatively charged protein surface [38]. This gives rise to an electrostatic steering effect which makes productive any collision of the substrate with the protein surface. In fact the negatively charged substrate is repulsed by the negatively charged protein surface and attracted by the positively charged active site [38]. In this regard, it must be noted that the C-terminal basic residues Lys24 and Arg25 of Cupricyclin-1 (Lys25 and Arg26 of Cupricyclin-2), according to the structural models obtained by MD simulations, are located on the opposite side of the copper solvent accessible site (Figure 3). These two residues could be substituted by negatively charged ones thus increasing the asymmetry of the electrosttstic potential distribution of the two peptides and their electrostatic steering effect on the substrate.

An additional issue that emerges from the results presented in this work is the difficulty in reconciling structural rigidity with the flexibility required to bind a metal ion in two different valence states. As stated in the Results and Discussion section, the imidazolate bridge that links the Cu and Zn ions in Cu,Zn SOD results in a distorted tetrahedral structure of the copper site which is crucial for high SOD activity [31,32]. The same geometry cannot be reproduced in our design making the copper environment in Cupricyclins significantly more rigid and resulting in a relatively low SOD activity. From this viewpoint, it is known that mononuclear metal centers based on iron, manganese and nickel display superoxide dismutase activity [39]. MnSOD, in particular, in which the metal ion is coordinated by one Asp and three His residues [39] appears to be a good model for future developments of our design. Further studies will be required to address this point and obtain high affinity metal binding peptides endowed with faster redox kinetics.

Materials and Methods

Molecular modelling

Initial structural models of Cupricyclin-1 and Cupricyclin-2 were built using the average solution structure of ω-conotoxin GVIA as a template (PDB code 2CCO [14]). The conformation of the inserted His residues was chosen using the standard Deep View rotamer library [40] so as to form a tetragonal metal binding site with geometry and ligand distances comparable to the copper binding site of bovine Cu,Zn superoxide dismutase (PDB code 2SOD [19]).

Molecular dynamics simulations

All simulations were performed with the GROMACS (v. 4.0.7) simulation package [41] together with the Amber99SB force field [42]. The parameter sets were generated by the *tleap* program of the Amber (v.9) molecular dynamics package [43]. The conversion into the GROMACS topology was performed by the Perl script *amb2gmx.pl* [44]. Lennard-Jones parameters ($R_{min}/2 = 1.0330$ Å, $\varepsilon = 0.0427$ kcal/mol) published by C. S. Babu and C. Lim were chosen for the copper ion [45].

Copper-coordinating residues (His8, His15, His19, His26 of Cupricyclin-1, and His8, His15, His20, His27 of Cupricyclin-2) were protonated at the Nδ1 position. Each molecule was placed in a rhombic dodecahedron box. The size of the simulation boxes was chosen to satisfy the condition that the distance between any protein atom and the box boundaries was larger than 1 nm. The simulation boxes were solvated with SPC/E [46] water molecules and neutralized with Cl^- ions. The solvated molecules were energy minimized by using the Steepest Descent algorithm until the convergence criterion of 100 kJ mol^{-1} nm^{-1} was reached (approx. 4000 steps for Cupricyclin-1 and 5100 steps for Cupricyclin-2). During the minimization runs position restraints of 1,000 kJ mol^{-1} nm^{-2} were applied to all non-hydrogen atoms of the proteins, except for copper-binding residues. The distances between the copper ion and the Nε2 atoms of the 4 coordinating histidine residues of each molecule were restrained to a value of 0.2 nm by using a harmonic potential of 100,000 kJ mol^{-1} nm^{-2} (bond type 6 of the GROMACS topology). 100 ps molecular dynamics simulation under NVT conditions, followed by 100 ps NPT simulation, with position restraints on all heavy atoms of the proteins and with restrained copper-ligand binding distances, were performed in order to equilibrate the temperature and pressure values of the systems. In the following two steps the structures were submitted to a 5 ns molecular dynamics simulation with harmonic potentials applied only to the distances between copper and its ligands and finally to a 10 ns simulation without any restraint.

A constant temperature value of 298 K was maintained during the simulations with the V-rescale algorithm [47], with a coupling constant of 0.1 ps. Parrinello-Rahman barostat [48] with a coupling constant of 2.0 ps was used for pressure coupling. The simulations were performed with a time step of 2 fs. Lennard-Jones interactions were cut off at 1.0 nm. Particle-mesh Ewald method (PME) [49] was applied to electrostatic interactions with a real space cutoff of 1.0 nm. All bonds, except those of water molecules, were constrained with the LINCS algorithm [50]. The SETTLE algorithm [51] was used for water molecules.

Peptides synthesis

Cupricyclins were synthesised by standard Fmoc chemistry on an automated Peptide Synthesizer (Pioneer, Applied Biosystems). The protected peptides were grown on a PAL-resin with a high level of modification, using the HATU/DIPEA amino acid activation, according to manufacturer's instructions. Side chain protection scheme was the following: Asp(*Ot*-Bu), Cys(Trt), Trp(Boc) and Lys(*t*-Boc). After synthesis, both peptides were released and deprotected by treatment with TFA/H_2O/triisopropylsilane (90:5:5 by volume) for 1 hr at room temperature. The cleavage mixture was filtered under vacuum into *t*-butyl-methyl ether at −20°C. Peptides were collected by centrifugation at 2500 rpm for 20 min at 4°C and washed with *t*-butyl-methyl ether. The pellet was dissolved in 50% acetonitrile and lyophilized. Peptides were loaded on a Vydac C_{18} semipreparative column (10 mm×250 mm, 5 μm particle size, 300 Å pore size) and isolated from by-products with an HPLC apparatus (model K1001, Knauer GmbH, Berlin, Germany), using a linear gradient of 5–80% acetonitrile, containing 0.2% TFA, in 60 min. Elution was monitored by absorbance at 230 nm with an on-line UV detector (model K2501, Knauer GmbH, Berlin, Germany) and peptide fractions were manually collected. The major peptide-containing fractions were air oxidized at 0.01% concentration (w/w) by magnetic stirring in 0.1 M NH_4HCO_3 for 30 min at room temperature. The cyclic peptides were finally purified from

dimers/multimers by HPLC, as described for purification of synthetic products (see above), and characterized by infusion in an electrospray mass spectrometry (ES-IT, mod. LCQ, ThermoElectron, San Jose, CA, USA).

Fluorescence quenching experiments

Fluorescence spectra of Cupricyclins were recorded at room temperarure with a Jasco FP-6200 spectrofluorometer. The excitation wavelength was 280 nm and the excitation and emission slits were set at 10 and 5 nm, respectively. Emission spectra were recorded in the 320 to 400 nm range. Peptides were dissolved at a concentration of 4.9×10^{-7} M in 50 mM sodium acetate buffer (pH 6.5). For copper binding studies, $CuCl_2$ (6.2×10^{-6} M) was added in aliquots and fluorescence was measured after 5 min after addition. The dissociation constant values given in the text are the average of at least three independent experiments.

Optical spectroscopy

UV-Vis electronic absorption spectra were recorded on an Perkin-Elmer λ14P spectrophotometer. Protein concentration was determined by UV absorption at 280 nm, by using a molar extinction coefficient (ε_{280}) of 8605 M^{-1} cm^{-1} [52].

EPR spectroscopy

Low temperature X-band EPR spectra were recorded on a Bruker ECS 106 spectrometer equipped with an ER4111VT temperature controller. In detail, spectra were recorded at 9.556 GHz and 115 K. Cupricyclins concentration was 0.5 mM in 50 mM sodium acetate buffer, pH 6.5.

NMR spectroscopy

NMR spectra were recorded at 300 K on a Bruker AVANCE AQS 600 spectrometer operating at 600.13 MHz and equipped with a Bruker multinuclear z-gradient probehead. Peptide solution was prepared in H_2O with 10% of D_2O (v/v). pH values of Cupricyclin-1 solution was adjusted to 8.0 by the addition of 0.1 M NaOH in D_2O to deprotonate the N-H/N-D group of the imidazole ring of histidine residues. In all the ^1H spectra, a soft presaturation of the HOD residual signal was applied.

Superoxide dismutase activity assay

Superoxide dismutase activity of Cupricyclins was determined using the pyrogallol enzymatic assay [34]. The assay was carried out at 30°C, in 20 mM Tris-HCl buffer pH 8.2, containing 1 mM EDTA and 200 μM pyrogallol, recording the absorption increase at 420 nm for 3 min. Bovine erythrocytes Cu,Zn superoxide dismutase (0.1 μM in 20 mM Tris HCl buffer pH 8.2) was used as a standard.

Supporting Information

Figure S1. Copper coordination environment in Cupricyclin-1 and Cu,Zn superoxide dismutase.
(DOC)

Figure S2 MALDI-TOF characterization of apo-Cupricyclin-1.
(DOC)

Figure S3 Differential Scanning Calorimetry analysis of Cupricyclin-1.
(DOC)

Figure S4 MALDI-TOF spectrum of holo-Cupricyclin-1.
(DOC)

Figure S5 MD simulations RMSD analysis of Cuprycyclin-1 and -2.
(DOC)

Acknowledgments

Authors wish to thank Dr. Maurizio Minetti for help in performing the EPR studies and Dr. Pasquale Stano and Dr. Cristiano Chiarabelli for helpful discussion.

Author Contributions

Conceived and designed the experiments: MB GM FP. Performed the experiments: MB APS VZ MCB LC MCS MES DP LM GM FP. Analyzed the data: MB APS VZ MCB LC MCS MES DP LM GM FP. Contributed reagents/materials/analysis tools: MCB LC MCS MES DP LM GM FP. Wrote the paper: MB GM FP. The paper was written with significant contributions from all authors: MB APS VZ MCB LC MCS MES DP LM GM FP.

References

1. Lu Y, Yeung N, Sieracki N, Marshall NM (2009) Design of functional metalloproteins. Nature 460: 855–862.
2. Jackel C, Kast P, Hilvert D (2008) Protein Design by Directed Evolution. Annu Rev Biophys 37: 153–173.
3. Berry SM, Lu Y (2011) Protein Structure Design and Engineering. In: Encyclopedia of Life Sciences (ELS) 1–8. John Wiley & Sons, Ltd: Chichester.
4. Kolmar H (2009) Biological diversity and therapeutic potential of natural and engineered cystine knot miniproteins. Curr Opin Pharmacol 9: 608–614.
5. Barba M, Sobolev AP, Romeo C, Schininà ME, Pietraforte D, et al. (2009) Cupryphans, metal-binding, redox-active, redesigned conopeptides. Prot Sci 18: 559–568.
6. Podtetenieff J, Taglieber A, Bill E, Reijerse EJ, Reetz MT (2010) An artificial metalloenzyme: creation of a designed copper binding site in a thermostable protein. Angew Chem Int Ed Engl 49: 5151–5155.
7. Gracy J, Le-Nguyen D, Gelly JC, Kaas Q, Heitz A, et al. (2008) KNOTTIN: the knottin or inhibitor cystine knot scaffold in 2007. Nucleic Acids Res 36: D314–D319.
8. Polticelli F, Pascarella S, Bordo D, Bolognesi M, Ascenzi P (1999) The T-knot motif revisited. Biol Chem 380: 1247–1250.
9. Olivera BM, Teichert RW (2007) Diversity of the neurotoxic Conus peptides: a model for concerted pharmacological discovery. Mol Interv 7: 251–260.
10. Raybaudi Massilia G, Schininà ME, Ascenzi P, Polticelli F (2001) Contryphan-Vn: a novel peptide from the venom of the Mediterranean snail *Conus ventricosus*. Biochem Biophys Res Commun 288: 908–913.
11. Raybaudi Massilia R, Eliseo T, Grolleau F, Lapied B, Barbier J, et al. (2003) Contryphan-Vn: a modulator of Ca2+-dependent K+ channels. Biochem Biophys Res Commun 303: 238–246.
12. Eliseo T, Cicero DO, Romeo C, Schininà ME, Raibaudy Massilia GR, et al. (2004) Solution structure of the cyclic peptide contryphan-Vn, a Ca2+-dependent K+ channel modulator. Biopolymers 74: 189–198.
13. Han TS, Teichert RW, Olivera BM, Bulaj G (2008) Conus venoms - a rich source of peptide-based therapeutics. Curr Pharm Des 14: 2462–2479.
14. Pallaghy PK, Norton RS (1999) Refined solution structure of omega-conotoxin GVIA: implications for calcium channel binding. J Pept Res 53: 343–351.
15. Schäffer A, Aravind L, Madden T, Shavirin S, Spouge J, et al. (2001) Improving the accuracy of PSI-BLAST protein database searches with composition-based statistics and other refinements. Nucleic Acids Res 29: 2994–3005.
16. Larkin M, Blackshields G, Brown N, Chenna R, McGettigan P, et al. (2007) Clustal W and Clustal X version 2.0. Bioinformatics 23: 2947–2948.
17. Crooks GE, Hon G, Chandonia JM, Brenner SE (2004) WebLogo: A sequence logo generator. Genome Research 14: 1188–1190.
18. Buczek O, Olivera BM, Bulaj G (2004) Propeptide does not act as an intramolecular chaperone but facilitates protein disulfide isomerase-assisted folding of a conotoxin precursor. Biochemistry 43: 1093–1101.
19. Tainer JA, Getzoff ED, Beem KM, Richardson JJ, Richardson DC (1982) Determination and analysis of the 2-Å-structure of copper,zinc superoxide dismutase. J Mol Biol 160: 181–217.
20. Polticelli F, Battistoni A, O'Neill P, Rotilio G, Desideri A (1998) Role of the electrostatic loop charged residues in Cu,Zn superoxide dismutase. Protein Sci 7: 2354–2358.
21. Vita C, Roumestand C, Toma F, Ménez A (1995) Scorpion toxins as natural scaffolds for protein engineering. Proc Natl Acad Sci 92: 6404–6408.
22. Cupane A, Leone M, Militello V, Stroppolo ME, Polticelli F, et al. (1994) Low-temperature optical spectroscopy of native and azide-reacted bovine Cu,Zn

superoxide dismutase. A structural dynamics study. Biochemistry 33: 15103–15109.
23. Bryce GF, Gurd FRN (1965) Visible spectra and optical rotatory properties of cupric ion complexes of L-histidine-containing peptides. J Biol Chem 241: 122–129.
24. Engeseth HR, McMillin DR (1986) Studies of thermally induced denaturation of azurin and azurin derivatives by differential scanning calorimetry: evidence for copper selectivity. Biochemistry 25: 2448–2455.
25. Sandberg A, Harrison DJ, Karlsson BG (2003) Thermal denaturation of spinach plastocyanin: effect of copper site oxidation state and molecular oxygen. Biochemistry 42: 10301–10310.
26. Shosheva A, Donchev A, Dimitrov M, Kostov G, Toromanov G, et al. (2005) Comparative study of the stability of poplar plastocyanin isoforms. Biochim Biophys Acta 1748: 116–127.
27. Peisach J, Blumberg WE (1974) Structural implications derived from the analysis of electron paramagnetic resonance spectra of natural and artificial copper proteins. Arch Biochem Biophys 165: 691–708.
28. Sakaguchi U, Addison AW (1979) Spectroscopic and redox studies of some copper(II) complexes with biomimetic donor atoms: implications for protein copper centers. J Am Chem Soc Dalton Trans 4: 600–608.
29. Beem KM, Rich WE, Rajagopalan KV (1974) Total reconstitution of copper-zinc superoxide dismutase. J Biol Chem 249: 7298–7305.
30. Pogni R, Baratto MC, Busi E, Basosi R (1999) EPR and O_2^- scavenger activity: Cu(II)-peptide complexes as superoxide dismutase models. J Inorg Biochem 73: 157–165.
31. Valentine JS, Doucette A, Potter SZ (2005) Copper-zinc superoxide dismutase and amyotrophic lateral sclerosis. Annu Rev Biochem 74: 563–593.
32. Roberts BR, Tainer JA, Getzoff ED, Malencik DA, Anderson SR, et al. (2007) Structural characterization of zinc-deficient human superoxide dismutase and implications for ALS. J Mol Biol 373: 877–890.
33. Jitsukawa K, Harata M, Arii H, Sakurai H, Masuda H (2001) SOD activities of the copper complexes with tripodal polypyridylamine ligands having a hydrogen bonding site. Inorg Chim Acta 324: 108–116.
34. Marklund S, Marklund G (1974) Involvement of the superoxide anion radical in the autoxidation of pyrogallol and a convenient assay for superoxide dismutase. Eur J Biochem 47: 469–474.
35. Rotilio G, Bray R, Fielden EM (1972) A pulse radiolysis of superoxide dismutase. Biochim Biophys Acta 286: 605–609.
36. Riley DP (1999) Functional Mimics of Superoxide Dismutase Enzymes as Therapeutic Agents. Chem Rev 99: 2573–2587.
37. Mejáre M, Bülow L (2001) Metal-binding proteins and peptides in bioremediation and phytoremediation of heavy metals. Trends Biotechnol 19: 67–73.
38. Desideri A, Falconi M, Polticelli F, Bolognesi M, Djinovic K, et al. (1992) Evolutionary conservativeness of electric field in the Cu,Zn superoxide dismutase active site. Evidence for co-ordinated mutation of charged amino acid residues. J Mol Biol 223: 337–342.
39. Miller AF (2004) Superoxide dismutases: active sites that save, but a protein that kills. Curr Opin Chem Biol 8: 162–168.
40. Guex N, Peitsch MC (1997) SWISS-MODEL and the Swiss-PdbViewer: An environment for comparative protein modelling. Electrophoresis 18: 2714–2723.
41. van der Spoel D, Lindahl E, Hess B, Groenhof G, Mark AE, et al. (2005) GROMACS: Fast, Flexible and Free. J Comp Chem 26: 1701–1718.
42. Wang J, Cieplak P, Kollman PA (2000) How well does a restrained electrostatic potential (RESP) model perform in calculating conformational energies of organic and biological molecules? J Comput Chem 21: 1049–1074.
43. Case DA, Darden TA, Cheatham TE, III, Simmerling CL, Wang J, et al. (2006) AMBER 9. University of California, San Francisco.
44. Mobley DL, Chodera JD, Dill KA (2006) On the use of orientational restraints and symmetry number corrections in alchemical free energy calculations. J Chem Phys 125: 084902.
45. Babu CS, Lim C (2006) Empirical force fields for biologically active divalent metal cations in water. J Phys Chem A 110: 691–699.
46. Berendsen HJC, Grigera JR, Straatsma TP (1987) The missing term in effective pair potentials. J Phys Chem 91: 6269–6271.
47. Bussi G, Donadio D, Parrinello M (2007) Canonical sampling through velocity rescaling. J Chem Phys 126: 014101.
48. Parrinello M, Rahman A (1981) Polymorphic transitions in single crystals: A new molecular dynamics method. J Appl Phys 52: 7182–7190.
49. Darden T, York D, Pedersen L (1993) Particle mesh Ewald: An N-log(N) method for Ewald sums in large systems. J Chem Phys 98: 10089–10092.
50. Hess B, Bekker H, Berendsen HJC, Fraaije JGEM (1997) LINCS: A linear constraint solver for molecular simulations. J Comp Chem 18: 1463–1472.
51. Miyamoto S, Kollman PA (1992) SETTLE: An analytical version of the SHAKE and RATTLE algorithms for rigid water models. J Comp Chem 13: 952–962.
52. Gill SC, von Hippel PH (1989) Calculation of protein extinction coefficents from aminoacid sequence data. Anal Biochem 182: 319–326.
53. Pettersen EF, Goddard TD, Huang CC, Couch GS, Greenblatt DM, et al. (2004) UCSF Chimera - A Visualization System for Exploratory Research and Analysis. J Comput Chem 25: 1605–1612.